International Journal of Engineering Research and General Science Volume 3, Issue 6, November-December, 2015
ISSN 2091-2730

EXACT SOLUTIONS FOR CHEMICALLY REACTIVE SPECIES IN CASSON FLUID PAST AN EXPONENTIALLY ACCELERATED SURFACE WITH NEWTONIAN HEATING IN THE PRESENCE OF THERMAL RADIATION

Preeti Jain*

*Department of Mathematics, University of Rajasthan

Jaipur-302004 (INDIA), M-9460500726

Abstract - An exact analysis of heat transfer accompanied by mass transfer flow of a Casson fluid past an exponentially accelerated infinite vertical plate with Newtonian heating in the presence of radiation is presented here. The governing coupled linear partial differential equations are transformed into linear ordinary differential equations by using non-dimensional variables. The resulting equations have been solved analytically using Laplace-transform technique. Closed form solutions are obtained for velocity, temperature and concentration profiles for different governing parameters. The paper intends to show unique results for a combination of heat transfer and chemical reaction in a Casson fluid flow. Expressions for shear stress in terms of Skin friction, the rate of heat transfer in terms of Nusselt number and mass transfer in terms of Sherwood number are also obtained. All the numerical results with various values of embedded flow parameters are analyzed graphically and their physical aspects are discussed in detail.

Keywords: Newtonian heating, Casson fluid, exponentially accelerated plate, unsteady free convection, Heat transfer, Mass transfer, thermal Radiation, Incompressible fluid.

MSC Classification: 76U, 76W, 76V, 76R, 65N.

Introduction

Newtonian fluids which have a linear relationship between the stress and the rate of strain are limited in view of their applications because they do not explain several technological applications for fluids in industry. Many complex fluids such as blood, clay coating, paints, honey, condensed milk, shampoos, soup, certain oils and greases, suspensions and many emulsions are noteworthy due to their various applications in the field of metallurgy, food processing, drilling operations, bioengineering operations and chemical and petroleum industries. In the literature they are known as non-Newtonian fluids. These fluids are described by a non-linear relationship between the stress and the rate of strain. In view of these applications and frequent occurrence of non-Newtonian fluids, the studies of such fluids have now become an increasingly appealing topic of current research in this field. The mechanics of non-Newtonian fluids present a special challenge to engineers, mathematicians and physicists. The Navier-Stokes theory is inadequate for describing such fluids and no single constitutive equation is available in the literature which exhibits the properties of all fluids. Because of the complexity of these fluids, there is not a single constitutive equation which exhibits all properties of such non-Newtonian fluids. Thus a number of non-Newtonian fluid models have been proposed to study their characteristic. The vast majority of non-Newtonian fluid models are concerned with simple models like the power law and grade two or three. These simple fluid models have short comings that render to results not having accordance with fluid flows in the reality (Mukhopadhyay and Vajravelu [1]). Power-law fluids models which are used to express non-Newtonian behavior in fluids predict shear thinning and shear thickening behavior. However it is inadequate in expressing normal stress behavior as observed in die swelling and rod climbing behavior in some non-Newtonian fluids. Normal stress effects can be expressed in second grade fluid model, a special type of Rivlin–Ericksen fluids, but this model is incapable of representing shear thinning/ thickening behavior (Aksoy et al. [2]). The non-Newtonian fluids are mainly classified into three types, namely differential, rate, and integral. The simplest subclass of the rate type fluids is the Maxwell model which can predict the stress relaxation. This rheological model, also, excludes the complicated effects of shear-dependent viscosity from any boundary layer analysis (Hayat et al. [3]). There is another type of non-Newtonian fluid known as Casson fluid. Casson [4] was the first who introduced this model for the prediction of the flow behavior of pigment oil suspensions used for preparation of printing inks. Casson fluid exhibits yield stress. It is well known that Casson fluid is a shear thinning liquid which is assumed to have an infinite viscosity at zero rate of shear, a yield stress below which no flow occurs, and a zero viscosity at an infinite rate of shear, i.e., if a shear stress less than the yield stress is applied to the fluid, it behaves like a solid, whereas if a shear stress greater than yield stress is applied, it starts to move. The examples of Casson fluid are jelly, tomato sauce, honey, soup, concentrated fruit juices, etc. Human blood can also be treated as Casson fluid. Due to the presence

of several substances like, protein, fibrinogen, and globulin in aqueous base plasma, human red blood cells can form a chain like structure, known as aggregates or rouleaux. If the rouleaux behave like a plastic solid, then there exists a yield stress that can be identified with the constant yield stress in Casson's fluid (Fung [5] and (Dash et al. [6]). Later on several researchers studied Casson fluid for different flow situations and configurations. Mustafa et al. [7] studied the unsteady boundary layer flow and heat transfer of a Casson fluid due to an impulsively started moving flat plate with a parallel free stream using homotopy analysis method (HAM). Mukhopadhyay [8-10] investigated Casson fluid flow and heat transfer over a nonlinearly stretching surface subjected to suction/blowing. The transformed equations were solved numerically by using the shooting method. Bhattacharya et al. [11, 12] analyzed the exact solution for boundary layer flow of Casson fluid over a permeable stretching/shrinking sheet.

Radiation effect plays an important role in various engineering processes. When the temperature of the surrounding fluid is rather high, radiation effects on the flow become significant. In some industrial applications such as glass production, furnace design, thermonuclear fusion, casting and levitation and in space technology applications such as cosmic flight aerodynamics, rocket propulsion systems, plasma physics, and space craft reentry aerothermodynamics which operate at higher temperature, radiation effects play an important role. Keeping in view this fact, Hossain et al. [13] determined the effect of radiation on the natural convection flow of an optically thick, viscous, incompressible flow past a heated vertical porous plate with a uniform surface temperature and a uniform rate of suction, where the radiation was included by assuming the Rosseland diffusion approximation. Raptis and Perdikis [14] studied the effects of thermal radiation and free convective flow past a uniformly accelerated vertical plate. Soundalgekar et al. [15] further presented exact solution to radiation effect on flow past an impulsively started vertical plate. Radiation effects on mixed convection along an isothermal vertical plate were studied by Hossain and Takhar [16]. Makinde [17] focused on the thermal radiation and mass transfer past a moving porous plate. Muthucumaraswamy [18, 19] obtained exact solutions taking into account the effects of thermal radiation under different boundary conditions. Recently, Deka and Das [20] investigated radiation effects past a vertical plate using ramped wall temperature, Jana and Ghosh [21] investigated radiative heat transfer in the presence of indirect natural convection. Numerical solutions of Casson fluid flow accompanied by heat transfer past an exponentially stretching surface in the presence of thermal radiation were presented by Pramanik [22].

The processes involving mass transfer effects are important in chemical processing equipments which are designed to draw high value products from cheaper raw materials with the involvement of chemical reaction. Mass transfer is important due to its applications in many scientific disciplines that involve convective transfer of atoms and molecules. Examples of this phenomenon are evaporation of water, separation of chemicals in distillation processes, natural or artificial sources etc. In addition, mass transfer with chemical reaction has special importance in chemical and hydrometallurgical industries. The formation of smog represents a first order homogeneous chemical reaction. For example, one can take into account the emission of NO_2 from automobiles and other smoke-stacks. NO_2 reacts chemically in the atmosphere with unburned hydrocarbons (aided by sunlight) and produces peroxyacetylnitrate, which forms a layer of photochemical smog (Shehzad [23]). Chemical reactions can be treated as either homogeneous or heterogeneous processes. It depends on whether they occur at an interface or as a single-phase volume reaction. A reaction is said to be of first order if the rate of reaction is directly proportional to the concentration itself which has many applications in different chemical engineering processes and other industrial applications such as polymer production, manufacturing of ceramics, and food processing A few representative studies dealing with mass transfer in the presence of chemical reaction may be mentioned. Das et al. [24] considered the effect of first order chemical reaction on the flow past an impulsively started infinite vertical plate with constant heat flux and mass transfer. Jain [25] investigated on the combined influence of Hall current and Soret effect on chemically reacting magneto-micropolar fluid flow from radiate rotating vertical surface with variable suction in slip-flow regime. Makanda et al. [26] studied the diffusion of chemically reactive species in Casson fluid flow over an unsteady stretching surface using Runge-Kutta-Fehlberg numerical scheme.

In all the studies cited above the flow is driven either by a prescribed surface temperature or by a prescribed surface heat flux. Here a different driving mechanism for unsteady free convection is considered; here the flow is set up by Newtonian heating from the surface. Heat transfer characteristic are dependent on the thermal boundary conditions. In general there are four common heating processes specifying the wall-to-ambient temperature distributions, prescribed surface heat flux distributions, conjugate conditions where heat is specified through a bounding surface of finite thickness and finite heat capacity. The interface temperature is not known a priori but depends on the intrinsic properties of the system, namely the thermal conductivity of the fluid and solid respectively. Newtonian heating, where the heat transfer rate from the bounding surface with a finite heat capacity is proportional to the local surface temperature and is usually termed conjugate convective flow. This configuration occurs in many important engineering devices, for example in heat exchangers where the conduction in solid tube wall is greatly influenced by the convection in the

fluid flowing over it. For conjugate heat transfer around fins where the conduction within the fin and the convection in the fluid surrounding it must be simultaneously analyzed in order to obtain the vital design information. In convective flows set up when the bounding surfaces absorbs heat by solar radiation. Therefore we conclude that the conventional assumption of no interaction of conduction-convection coupled effects is not always realistic and it must be considered when evaluating the conjugate heat transfer processes in many practical engineering applications. Merkin [27] was the first to consider the free-convection boundary-layer over a vertical flat plate immersed in a viscous fluid whilst [28, 29, 30] considered the cases of vertical and horizontal surfaces embedded in a porous medium. The studies mentioned in [27 - 30] deal with steady free convection. In this area, the authors of this paper, Jain and Chaudhary [31, 32] were the first one to give exact solution to the unsteady free convection boundary-layer flow from a flat vertical plate with Newtonian heating and the solution was obtained in closed-form using Laplace transform technique. Recently, Jain [33] presented exact solution of heat and mass transfer past an inclined oscillating surface with Newtonian heating under the effect of thermal radiation and mass diffusion. Our work was further extended by Narahari and Nayan [34], Raju et al. [35], Narahari and Ishak [36] and Hussanan et al. [37] in which they incorporated the effects of thermal radiation and mass transfer with Newtonian heating under different boundary conditions like impulsively started plate, oscillating plate, moving plate etc. An exact solution of the unsteady free convection flow of a viscous incompressible, optically thin, radiating fluid past an impulsively started vertical porous plate with Newtonian heating was investigated by Mebine and Adigio [38].

To the best of author's knowledge, so far, no study has been reported in the literature which investigates the unsteady free convection flow of chemically reactive species in Casson fluid past an exponentially accelerated plate with Newtonian heating accompanied by heat and mass transfer in the presence of thermal radiation. In this study, the equations of the problem are first formulated and transformed into their dimensionless forms where the Laplace transform method is applied to find the exact solutions for velocity, temperature and concentration. Furthermore, expressions for skin friction, Nusselt number and Sherwood number are obtained and are plotted graphically and discussed for the pertinent flow parameters. Exact solutions obtained in this paper are important not only because do they correspond to some fundamental flow application but also they are useful for explaining the physical aspects of the flow problem in detail. More over exact solutions are being used as a benchmark for validation of other solutions obtained via approximate or numerical schemes.

Mathematical Analysis

Let us consider the effect of Newtonian heating on unsteady free convection flow of a viscous, incompressible Casson fluid past an infinite vertical flat plate. The x^*-axis is taken along an infinite vertical plate and parallel to the free stream velocity and y^*-axis is taken normal to it. It is assumed that initially at time $t^* = 0$, the plate and fluid are at rest with constant temperature T_∞^* and concentration level C_∞^* at all points. At time $t^* \geq 0$, suddenly the plate is accelerated with velocity $\exp(a_0^* t^*)$ in its own plane along the x^*- axis against the gravitational field and the rate of heat transfer from the surface is proportional to the local surface temperature T^*, also the concentration level near the plate is raised from C_∞^* to C_w^*. It is also assumed that there exists a homogeneous chemical reaction of first order with constant rate K_c between the diffusing species and the fluid. Since the plate is infinite in the x^* direction therefore all the flow variables are independent of x^* and are functions of y^* and t^* only. The fluid is considered to be gray absorbing-emitting radiation and non-scattering medium. We assume that the rheological equation of state for an isotropic and incompressible flow of a Casson fluid can be written as (Mukhopadhyay [9])

$$\tau_{ij} = \begin{cases} 2\left(\mu_B + p_y / \sqrt{2\pi}\right) e_{ij} & , \quad \pi > \pi_c \\ 2\left(\mu_B + p_y / \sqrt{2\pi}\right) e_{ij} & , \quad \pi < \pi_c \end{cases}$$

where $\pi = e_{ij} e_{ij}$ and e_{ij} is the $(i, j)^{th}$ component of the deformation rate so π is the product of the component of deformation rate with itself, π_c is a critical value of this product based on the non-Newtonian model, μ_B is plastic dynamic viscosity of the non-Newtonian fluid, and p_y is yield stress of fluid. So if a shear stress less than the yield stress is applied to the fluid, it behaves like a solid, whereas if a shear tress greater than the yield stress is applied, it starts to move.

It is also assumed that the viscous dissipation term in the energy equation and the heat produced by chemical reaction is negligible, as the fluid velocity is low. Under these conditions along with the assumptions, we apply the Boussinesq approximation which states that all fluid properties are constant with the exception of the density variation in the buoyancy term, the free convective problem is governed by the following set of partial differential equations:-

$$\rho\frac{\partial u^*}{\partial t^*} = \mu_B\left(1+\frac{1}{\beta}\right)\frac{\partial^2 u^*}{\partial y^{*2}} + \rho g\,\beta_t\,(T^* - T_\infty^*) + \rho g\,\beta_c\,(C^* - C_\infty^*) \quad \ldots(1)$$

$$\rho\, c_p\,\frac{\partial T^*}{\partial t^*} = k\frac{\partial^2 T^*}{\partial y^{*2}} - \frac{\partial q_r}{\partial y^*} \quad \ldots(2)$$

$$\frac{\partial C^*}{\partial t^*} = D\,\frac{\partial^2 C^*}{\partial y^{*2}} - K_c C^* \quad \ldots(3)$$

With the following initial and boundary conditions:

$$\left.\begin{aligned} &t^* \le 0 : u^* = 0, \quad T^* = T_\infty^*, \quad C^* = C_\infty^* \qquad \text{for all } y^* > 0 \\ &t^* > 0 : u^* = \exp(a_0^* t^*), \quad \frac{\partial T^*}{\partial y^*} = -\frac{h}{k}\,T^*,\ C^* = C_w^* \text{ at } y^* = 0 \\ &\qquad\quad : u^* = 0, \qquad T^* \to T_\infty^*, C^* \to C_\infty^* \qquad \text{as } y^* \to \infty \end{aligned}\right\} \quad \ldots(4)$$

The radiation heat flux under Rosseland's approximation [39] is expressed by

$$q_r = -\frac{4\sigma}{3k^*}\frac{\partial^4 T^*}{\partial y^*} \quad \ldots(5)$$

This model is valid for optically-thick media in which thermal radiation propagates only a limited distance prior to experiencing scattering or absorption. The local thermal radiation intensity is due to radiation emanating from proximate locations in the vicinity of which emission and scattering are comparable to the location of interest. For zones where conditions are appreciably different thermal radiation has been shown to be greatly attenuated before arriving at the location under consideration. The energy transfer depends on conditions only in the area adjacent to the plate regime i.e. the boundary layer regime. Rosseland's model yields accurate results for intensive absorption i.e. optically-thick flows which are optically far from the bounding surface. It is assumed that the temperature differences within the flow are sufficiently small and then (5) can be linearized by expanding T^{*4} into Taylor series about T_∞^*, which after neglecting higher order terms takes the form:

$$T^{*4} \cong 4T_\infty^{*3}T^* - 3T_\infty^{*4} \quad \ldots(6)$$

In view of (5) and (6), (2) reduces to

$$\rho C_p\,\frac{\partial T^*}{\partial t^*} = \left(k + \frac{16\sigma T_\infty^{*3}}{3k^*}\right)\frac{\partial^2 T^*}{\partial y^{*2}} \quad \ldots(7)$$

To reduce the above equations into their non-dimensional forms, we introduce the following non-dimensional quantities:-

$$\left.\begin{aligned} u &= \frac{u^*}{U_0},\ t = \frac{t^* U_0^2}{\nu},\ y = \frac{y^* U_0}{\nu},\ a_0 = \frac{a_0^* \nu}{U_0^2} \\ \theta &= \frac{T^* - T_\infty^*}{T_\infty^*},\ C = \frac{C^* - C_\infty^*}{C_W^* - C_\infty^*},\ Pr = \frac{\mu C_p}{k},\ Sc = \frac{\nu}{D} \\ Gr &= \frac{\nu g \beta_t T_\infty^*}{U_0^3},\ Gm = \frac{\nu g \beta_c (C_W^* - C_\infty^*)}{U_0^3},\ R = \frac{16\sigma T_\infty^{*3}}{3k k^*} \\ \beta &= \frac{\mu_B \sqrt{2\pi_c}}{p_y},\quad \gamma = \frac{h\nu}{kU_0},\quad \alpha = \frac{K_c \nu}{U_0^2} \end{aligned}\right\} \quad \ldots(8)$$

Substituting the transformation (8) into equations (1), (3) and (7), we obtain the following non-dimensional partial differential equations:

$$\frac{\partial u}{\partial t} = \left(1 + \frac{1}{\beta}\right)\frac{\partial^2 u}{\partial y^2} + Gr\,\theta + Gm\,C \quad \ldots(9)$$

$$Pr \frac{\partial \theta}{\partial t} = (1+R)\frac{\partial^2 \theta}{\partial y^2} \quad \ldots(10)$$

$$\frac{\partial C}{\partial t} = \frac{1}{Sc}\frac{\partial^2 C}{\partial y^2} - \alpha C \quad \ldots(11)$$

The corresponding initial and boundary conditions in non-dimensional form are:

$$\left.\begin{aligned} t \le 0 &: u = 0,\ \theta = 0,\ C = 0 \quad \text{for all } y > 0 \\ t > 0 &: u = \exp(a_0 t),\ \frac{\partial \theta}{\partial y} = -\gamma(1+\theta),\ C = 1 \text{ at } y = 0 \\ &: u \to 0,\ \theta \to 0, C \to 0 \quad \text{as } y \to \infty \end{aligned}\right\} \quad \ldots(12)$$

Where,

$\gamma = \frac{h\nu}{kU_0}$ is the Newtonian heating parameter, when $\gamma = 0$ then $\theta = 0$ which physically corresponds that no heating from the plate exists [40, 41]. Radiation parameter (R) embodies the relative contribution of heat transfer by thermal radiation to thermal conduction. Large R (>1) values therefore correspond to thermal radiation dominance and small values (<1) to thermal conduction dominance (Siegel and Howell [42]). For R = 1 both conduction and radiative heat transfer modes will contribute equally to the regime. Clearly the term in r. h. s. of (10) is an augmented diffusion term i.e. with R = 0, thermal radiation vanishes and equation (10) reduces to the familiar unsteady one-dimensional conduction-convection equation. Rests of the physical variables are defined in Nomenclature.

Analytical solutions by the Laplace transform method

The thermal and concentration equations (10) and (11) are uncoupled from the momentum equation (9). One can therefore solve for the temperature variable θ(y, t) and concentration variable C(y, t) whereupon the solution of u(y, t) can also be obtained, using Laplace transform technique. The Laplace transform method solves differential equations and corresponding initial and boundary value problems. The Laplace transform has the advantage that it solves initial value problems directly without determining first a general solution and non-homogeneous

differential equations without solving first the corresponding homogeneous equations. Applying the Laplace transform with respect to time t to the eqs. (9) - (11) we get,

$$\left.\begin{aligned} q\,\bar{u}(y,q)-u(y,0)&=\left(1+\frac{1}{\beta}\right)\frac{d^2\bar{u}(y,q)}{dy^2}+Gr\;\bar{\theta}(y,q)+Gm\;\bar{C}(y,q)\\ Pr\left[q\,\bar{\theta}(y,q)-\theta(y,0)\right]&=(1+R)\frac{d^2\bar{\theta}(y,q)}{dy^2}\\ Sc\left[q\,\bar{C}(y,q)-C(y,0)\right]&=\frac{d^2\bar{C}(y,q)}{dy^2}-\alpha Sc\;\bar{C}(y,q)\end{aligned}\right\} \quad \ldots(13)$$

Here,

$\bar{u}(y,q)=\int_0^\infty e^{-qt}u(y,t)dt,\ \bar{\theta}(y,q)=\int_0^\infty e^{-qt}\theta(y,t)dt$ and $\bar{C}(y,q)=\int_0^\infty e^{-qt}C(y,t)dt$ denotes the Laplace transforms of $u(y,t),\ \theta(y,t)$ and $C(y,t)$ respectively.

Using the initial condition (12), we get

$$\frac{d^2\bar{u}(y,q)}{dy^2}-\left(\frac{1+\beta}{\beta}\right)q\,\bar{u}(y,q)+\frac{Gr\,\beta}{1+\beta}\;\bar{\theta}(y,q)+\frac{Gm\,\beta}{1+\beta}\;\bar{C}(y,q)=0 \quad \ldots(14)$$

$$\frac{d^2\bar{\theta}(y,q)}{dy^2}-q\left(\frac{Pr}{1+R}\right)\bar{\theta}(y,q)=0 \quad \ldots(15)$$

$$\frac{d^2\bar{C}(y,q)}{dy^2}-\left(\alpha Sc+q\,Sc\right)\bar{C}(y,q)=0 \quad \ldots(16)$$

The corresponding transformed boundary conditions are:

$$\left.\begin{aligned} &t>0:\ \bar{u}(y,q)=\frac{1}{q-a_0},\ \frac{d\bar{\theta}(y,q)}{dy}=-\gamma\left[\frac{1}{q}+\bar{\theta}(y,q)\right],\ \bar{C}(y,q)=\frac{1}{q}\ \text{at}\ y=0\\ &\bar{u}(y,q)\to 0,\ \bar{\theta}(y,q)\to 0,\ \bar{C}(y,q)\to 0\quad \text{as}\ y\to\infty\end{aligned}\right\} \quad \ldots(17)$$

The solutions of (14) – (16) subject to the boundary conditions (17) are:

$$\bar{u}(y,q)=\frac{1}{(q-a_0)}e^{-y\sqrt{a}\sqrt{q}}+\frac{Gr\,a\,c}{Pr_{eff}-a}\frac{1}{q^2(\sqrt{q}-c)}e^{-y\sqrt{a}\sqrt{q}}-\frac{Gm\,a}{\alpha Sc}\left[\frac{1}{(q-b)}e^{-y\sqrt{a}\sqrt{q}}-\frac{1}{q}e^{-y\sqrt{a}\sqrt{q}}\right]$$
$$-\frac{Gr\,a\,c}{Pr_{eff}-a}\frac{1}{q^2(\sqrt{q}-c)}e^{-y\sqrt{Pr}\sqrt{q}}+\frac{Gm\,a}{\alpha Sc}\left[\frac{1}{(q-b)}e^{-y\sqrt{Sc}\sqrt{q+\alpha}}-\frac{1}{q}e^{-y\sqrt{Sc}\sqrt{q+\alpha}}\right] \quad \ldots(18)$$

$$\bar{\theta}(y,q)=\frac{c}{q(\sqrt{q}-c)}e^{-y\sqrt{q\,Pr_{eff}}} \quad \ldots(19)$$

$$\overline{C}(y,q)=\frac{1}{q}e^{-y\sqrt{(\alpha+q)Sc}} \quad \ldots(20)$$

Where,

$a=\frac{\beta}{1+\beta}, b=\frac{\alpha Sc}{a-Sc}, c=\frac{\gamma}{\sqrt{Pr_{eff}}}$ and $Pr_{eff}=\frac{Pr}{1+R}$, Pr_{eff} is the effective Prandtl number.

By taking the inverse Laplace transform of equations (18) – (20) the solutions are derived as:

$$\theta(y,t)=F_1(y\sqrt{Pr_{eff}},\ c,\ t) \quad \ldots(21)$$

$$C(y,t)=F_2(y\sqrt{Sc},\ \alpha,t) \quad \ldots(22)$$

$$u(y,t)=F_3(y\sqrt{a},a_0,t)+\frac{Gr\,a\,c}{Pr_{eff}-a}\left[F_4(y\sqrt{a},c,t)-F_4(y\sqrt{Pr_{eff}},c,t)\right]$$
$$-\frac{Gm\,a}{\alpha Sc}\left[F_3(y\sqrt{a},b,t)-F_5(y\sqrt{a},t)\right]+\frac{Gm\,a}{\alpha Sc}\left[F_6(y\sqrt{Sc},\alpha,b,t)-F_2(y\sqrt{Sc},\alpha,t)\right] \quad \ldots(23)$$

Here,

$$F_1(z_1,z_2,t)=L^{-1}\left(\frac{1}{q(\sqrt{q}-z_2)}e^{-z_1\sqrt{q}}\right)=e^{\left(z_2^2t-z_1z_2\right)}\operatorname{erfc}\left(\frac{z_1}{2\sqrt{t}}-z_2\sqrt{t}\right)-\operatorname{erfc}\left(\frac{z_1}{2\sqrt{t}}\right) \quad \ldots(24)$$

$$F_2(z_1,z_2,t)=L^{-1}\left(\frac{1}{q}e^{-z_1\sqrt{q+z_2}}\right)=\frac{1}{2}\left[e^{z_1\sqrt{z_2}}\operatorname{erfc}\left(\frac{z_1}{2\sqrt{t}}+\sqrt{z_2t}\right)+e^{-z_1\sqrt{z_2}}\operatorname{erfc}\left(\frac{z_1}{2\sqrt{t}}-\sqrt{z_2t}\right)\right] \quad \ldots(25)$$

$$F_3(z_1,z_2,t)=L^{-1}\left(\frac{1}{q-z_2}e^{-z_1\sqrt{q}}\right)=\frac{e^{z_2t}}{2}\left[e^{z_1\sqrt{z_2}}\operatorname{erfc}\left(\frac{z_1}{2\sqrt{t}}+\sqrt{z_2t}\right)+e^{-z_1\sqrt{z_2}}\operatorname{erfc}\left(\frac{z_1}{2\sqrt{t}}-\sqrt{z_2t}\right)\right] \quad \ldots(26)$$

$$F_4(z_1,z_2,t)=L^{-1}\left(\frac{1}{q^2(\sqrt{q}-z_2)}e^{-z_1\sqrt{q}}\right)=\frac{1}{z_2^3}\left[e^{\left(z_2^2t-z_1z_2\right)}\operatorname{erfc}\left(\frac{z_1}{2\sqrt{t}}-\sqrt{z_2t}\right)-\operatorname{erfc}\left(\frac{z_1}{2\sqrt{t}}\right)\right]$$
$$-\frac{1}{z_2}\left[\left(t+\frac{z_1^2}{2}\right)\operatorname{erfc}\left(\frac{z_1}{2\sqrt{t}}\right)-z_1\sqrt{\frac{t}{\pi}}e^{-\left(z_1/2\sqrt{t}\right)^2}\right]-\frac{1}{z_2^2}\left[2\sqrt{\frac{t}{\pi}}e^{-\left(z_1/2\sqrt{t}\right)^2}-z_1\operatorname{erfc}\left(\frac{z_1}{2\sqrt{t}}\right)\right] \quad \ldots(27)$$

$$F_5(z_1,\ t)=L^{-1}\left(\frac{1}{q}e^{-z_1\sqrt{q}}\right)=\operatorname{erfc}\left(\frac{z_1}{2\sqrt{t}}\right) \quad \ldots(28)$$

$$F_6(z_1, z_2, z_3, t) = L^{-1}\left(\frac{1}{q - z_3} e^{-z_1\sqrt{q+z_2}}\right) =$$

$$\frac{e^{z_3 t}}{2}\left[e^{z_1\sqrt{z_2+z_3}}\,\mathrm{erfc}\left(\frac{z_1}{2\sqrt{t}} + \sqrt{(z_2+z_3)t}\right) + e^{-z_1\sqrt{z_2+z_3}}\,\mathrm{erfc}\left(\frac{z_1}{2\sqrt{t}} - \sqrt{(z_2+z_3)t}\right)\right]$$

…(29)

erfc (x) being the complementary error function defined by

$$\mathrm{erfc}(x) = 1 - \mathrm{erf}(x),\ \mathrm{erf}(x) = \frac{2}{\sqrt{\pi}}\int_0^x \exp(-\eta^2)\,d\eta$$

$$\mathrm{erfc}(0) = 1,\ \mathrm{erfc}(\infty) = 0.$$

Also z_1, z_2, z_3 are dummy variables and F_1, F_2, F_3, F_4, F_5 and F_6 are dummy function. The solution of the problem introduced new inverse Laplace transforms of exponential forms which are not available in the literature. These formulas are derived and are provided in the solution.

Limiting Case

The solutions obtained above are more general. If $\beta \to \infty$, the solution for velocity given in equation (23) reduces to the corresponding solution for Newtonian fluid given by:

$$u(y,t) = F_3(y, a_0, t) + \frac{Gr\ c}{Pr_{eff} - 1}\left[F_4(y, c, t) - F_4(y\sqrt{Pr_{eff}}, c, t)\right]$$

$$-\frac{Gm}{\alpha Sc}\left[F_3(y, b, t) - F_5(y, t)\right] + \frac{Gm}{\alpha Sc}\left[F_6(y\sqrt{Sc}, \alpha, d, t) - F_2(y\sqrt{Sc}, \alpha, t)\right]$$

$$\text{Where}\quad d = \frac{\alpha Sc}{1 - Sc} \qquad \text{....(30)}$$

Skin-friction

Knowing the velocity field, we now study the changes in the skin-friction. It is given by:- $\tau^* = -\mu\left(1 + \frac{1}{\beta}\right)\left(\frac{\partial u^*}{\partial y^*}\right)_{y^*=0}$

…(31)

The dimensionless expression for skin-friction evaluated using (23) is given by:

$$\tau = \frac{\tau^*}{\rho U_0^2} = -\left(1 + \frac{1}{\beta}\right)\left(\frac{\partial u}{\partial y}\right)_{y=0} \qquad \text{…(32)}$$

$$\tau = \frac{\tau^*}{\rho U_0^2} = -\frac{1}{a}\left(\frac{\partial u}{\partial y}\right)_{y=0}$$

$$= -\frac{1}{a}\left\{-\sqrt{\frac{a}{\pi t}} - \sqrt{aa_o}\,\mathrm{erf}\left(\sqrt{a_0 t}\right) - \left(\frac{Gr\,a\,c}{Pr_{eff} - a}\right)\left\{\frac{1}{c^3}\left[-\sqrt{\frac{a}{\pi t}} + e^{tc^2}\,c\sqrt{a}\left(1 + \mathrm{erf}\left(\sqrt{ct}\right)\right) + e^{tc^2 - tc}\sqrt{\frac{a}{\pi t}}\right]\right.\right.$$

$$\left.\left. - \frac{2}{c}\sqrt{\frac{a\,t}{\pi}} - \frac{\sqrt{a}}{c^2}\right\} + \frac{Gm\,a}{\alpha Sc}\left\{e^{ft}\sqrt{af}\;\mathrm{erf}\left(\sqrt{ft}\right)\right\}\right.$$ **Nusselt number**

$$\left. + \left(\frac{Gr\,a\,c}{Pr_{eff} - a}\right)\left\{\frac{1}{c^3}\left[-\sqrt{\frac{Pr}{\pi t}} + e^{tc^2}\,c\sqrt{Pr}\left(1 + \mathrm{erf}\left(\sqrt{ct}\right)\right) + e^{tc^2 - tc}\sqrt{\frac{Pr}{\pi t}}\right] - \frac{2}{c}\sqrt{\frac{Pr\,t}{\pi}} - \frac{\sqrt{Pr}}{c^2}\right\}\right.$$

$$\left. - \frac{Gm\,a}{\alpha Sc}\left\{e^{ft}\sqrt{Sc(f+\alpha)}\;\mathrm{erf}\left(\sqrt{(f+\alpha)t}\right)\right\} + \frac{Gm\,a}{\alpha Sc}\left\{\sqrt{\alpha Sc}\;\mathrm{erf}\left(\sqrt{\alpha t}\right)\right\}\right\} \qquad \ldots(33)$$

Another phenomenon in this study is to understand the effects of t and Pr on Nusselt number. The rate of heat transfer in non-dimensional form as calculated from the temperature field (21) is given by:-

$$Nu = -\frac{\upsilon}{U_0\left(T^* - T_\infty^*\right)}\left.\frac{\partial T^*}{\partial y^*}\right|_{y^*=0} = \frac{1}{\theta(0)} + 1$$

$$= c\sqrt{Pr_{eff}}\left(1 + \frac{1}{e^{c^2 t}\left[1 + \mathrm{erf}\left(c\sqrt{t}\right)\right] - 1}\right) \qquad \ldots (34)$$

Sherwood number

The rate of concentration transfer in non-dimensional form as calculated from the concentration field (22) is given by:-

$$Sh = -\left.\frac{\partial C}{\partial y}\right|_{y=0} = \sqrt{\frac{\alpha Sc}{2}}\left(2 + \frac{1}{2}\sqrt{\frac{Sc}{t}}\;e^{-\alpha t}\right) \qquad \ldots(35)$$

Discussion and Conclusion

In order to get a clear understanding of the effects of various physical parameters on the velocity field, thermal boundary layer, concentration boundary layer, skin-friction, Nusselt number and Sherwood number of a Casson fluid, a detailed numerical computation of the closed form analytical solutions (obtained in the preceding section) have been carried out and shown graphically. The regime is controlled by several thermo-physical parameters which are Casson parameter (□), radiation parameter (R), Prandtl number (Pr), Grashof number (Gr), modified Grashof number (Gm), Schmidt number (Sc), Newtonian heating parameter (γ), chemical reaction parameter (□), exponential accelerated parameter (a_0) and time (t).

In figure 1 the development of dimensionless temperature profiles θ(y, t) inside the boundary layer against span wise coordinate y for different values of Boltzmann-Rosseland radiation parameter (R) is shown. Again Pr = 0.71 i.e. Pr < 1, so that heat diffuses faster than momentum in the regime. $R = \frac{16\sigma T_\infty^{*3}}{3k\,k^*}$ corresponds to the relative contribution of thermal radiation heat transfer to thermal conduction heat transfer. For

R<<1, thermal conduction heat transfer will dominate and vice versa for R > 1. Larger values of R therefore physically correspond to stronger thermal radiation flux and in accordance with this, the maximum temperatures are observed for R = 2. Rosseland's radiation diffusion model effectively enhances the thermal diffusivity, as described by Siegel and Howell. From this figure it is depicted that an increase in radiation parameter leads to an increase in the temperature in the boundary layer region which implies that radiation tends to enhance fluid temperature. Figure 2 exhibits the influence of dimensionless time t on the thermal boundary layer θ(y, t). It is observed that there is an enhancement in fluid temperature as time progresses.

Figure 3 illustrates the influence of Prandtl number (Pr) on fluid temperature taking Pr = 0.71, 1.0, 7.0 and 3 which physically corresponds to air, electrolytic solution, water and Freon CCl_2F_2 respectively at 20^0C temperature and 1 atmospheric pressure. It is inferred that the thickness of thermal boundary layer is greatest for Pr = 0.71 (air), then for Pr = 1.0 (electrolytic solution) and then for Pr = 7.0 (water) and finally lowest for Pr = 3 (Freon) i.e. an increase in the Prandtl number results in a decrease of temperature. An increase in Prandtl number reduces the thermal boundary layer thickness. Pr signifies the relative effects of viscosity to thermal conductivity. In heat transfer problems, the Prandtl number Pr controls the relative thickening of the momentum and thermal boundary layers. Fluids with lower Prandtl number have higher thermal conductivities (and thicker thermal boundary layer structures) and therefore heat can diffuse from the sheet faster than for higher Prandtl number fluids (thinner boundary layers). Hence, Prandtl number can be used to increase the rate of cooling in conducting flows. s

From figure 4 it is reported that an increase in the Newtonian heating parameter (γ) the thermal boundary layer thickness also increases and as a result the surface temperature of the plate increases. From figures 1 to 4 it is found that the maximum of the temperature occur in the vicinity of the plate and asymptotically approaches to zero in the free stream region. The graphical behavior of temperature represented in figures 1 - 4 are in good agreement with the corresponding boundary conditions of temperature profiles as shown in equation (12).

In Figure 5 the concentration profiles C(y,t) are shown for different values of the Schmidt number (Sc) and time (t) respectively. Different values of Schmidt number Sc = 0.22, 0.30, 0.66, 0.78 and 0.94 are chosen which physically correspond to Hydrogen, Helium, Oxygen, Ammonia and Carbon dioxide respectively at 25^0C temperature and 1 atmospheric pressure. The profiles have a common feature that the concentration decreases exponentially from the surface to zero value far away in the free stream. A comparison of curves in the figures show that the concentration boundary layer decreases with increasing Schmidt number while it enhances for increasing times. This is consistent with the fact that an increase in Sc means decrease of molecular diffusivity that result in decrease of concentration boundary layer. Hence, the concentration of species is higher for small values of Sc and lower for large values of Sc. Effects of Chemical reaction parameter (□) are displayed in figure 6 and it is observed that an increase in the values of the chemical reaction parameter the thickness of concentration profiles C(y,t) decreases. When □ = 0, there is no chemical reaction. An increase in the chemical reaction parameter corresponds to an increase in the reaction rate parameter and an increase in the reaction rate parameter results in reduction in concentration boundary layer.

The effects of Grashof number (Gr) and modified Grashof number (Gm) on velocity profiles are exhibited in figure 7. The trend shows that the velocity enhances with increasing values of Gr and Gm. The figure reveals that the maximum velocity is attained near the plate and approaches to zero far away from the plate. Physically this is possible because as the Grashof number and modified Grashof number increases, the contribution from the thermal and mass buoyancy near the plate becomes significant and hence a rise in the velocity near the plate is observed. This gives rise to an increase in the induced flow. For higher values of Gr, the fluid velocity overshoots the plate velocity in the regions close to the boundary which means that maximum velocity occurs in the fluid close to the surface but not at the surface. Here Gr = 0 and Gm = 0 corresponds to the absence of free convection and mass buoyancy effect respectively.

The velocity profiles u(y, t) illustrating the effects of radiation parameter (R) are shown in Figure 8. It is revealed from this figure that the radiation parameter R has an accelerating influence on fluid flow. Physically, it is due to the fact that an increase in the radiation parameter R for fixed values of other parameters decreases the rate of radiative heat transfer to the fluid, and consequently, the fluid velocity increases.

The graphical results for the influence of Casson fluid parameter (□) on the flow field are depicted in figure 9. The effect of increasing values of Casson fluid parameter is to reduce the velocity and hence the boundary layer thickness decreases. Increasing values of Casson parameter

imply decreasing yield stress so the fluid behaves as Newtonian fluid as Casson parameter becomes large. When □ → ∞ the non-Newtonian behaviors disappear and the fluid purely behaves like a Newtonian fluid. Thus, the velocity boundary layer thickness for Casson fluid is larger than the Newtonian fluid. It happens because of plasticity of Casson fluid. As Casson parameter decreases, the plasticity of the fluid increases which produces an increment in velocity boundary layer thickness.

Figure 10 displays the effects of Schmidt number Sc on the velocity field. It is inferred that the velocity decreases with increasing Schmidt number. An increasing Schmidt number implies that viscous forces dominate over the diffusion effects. Schmidt number in free convection flow regimes represents the relative effectiveness of momentum and mass transport by diffusion in the velocity (momentum) and concentration (species) boundary layers. Smaller Sc values correspond to lower molecular weight species diffusing in air (e.g. Hydrogen (Sc = 0.16), Helium (Sc = 0.3), water vapour (Sc = 0. 6), oxygen (Sc = 0.66)) and higher values to denser hydrocarbons diffusing in air. Effectively therefore an increase in Sc will counteract momentum diffusion since viscosity effects will increase and molecular diffusivity will be reduced. The flow will therefore be decelerated with a rise in Sc as testified by figure 10. It is also important to note that for Sc ~ 1, the velocity and concentration boundary layers will have the same thickness. For Sc < 1 species diffusion rate greatly exceeds the momentum diffusion rate and vice versa for Sc > 1.

The effect of temporal variable t and Prandtl number (Pr) on the flow field are presented in figure 11 and it is revealed that as the time progresses the thickness of momentum boundary layer increases while reverse happens for increasing values of Prandtl number. It is evident from the figure that the fluid velocity overshoots the plate velocity in the regions close to the boundary. This overshooting is more pronounced for low Prandtl number fluids than for higher Prandtl number fluids. Also the thickness of momentum boundary layer is more for fluid with low Prandtl number. The reason underlying this behavior arises from the fact that the fluids with high Prandtl number have high viscosity, which makes the fluid thick and hence the fluid moves slowly.

Figure 12 displays the effect of Newtonian heating parameter (γ) on the dimensionless velocity. It is observed that as the conjugate parameter for Newtonian heating increases the density of the fluid decreases, and the momentum boundary layer thickness increases and as a result the velocity increases within the boundary layer. For higher values of γ the fluid velocity overshoots the plate velocity in the regions close to the boundary.

From figure 13 it is noticed that chemical reaction parameter (□) decreases the velocity of the fluid. The decrease is attributed to the absorption of heat energy due to endothermic reaction (γ > 0). Further the presence of heavier diffusing species causes a decrease in velocity leading to thinning of the boundary layer thickness. The effect of exponential accelerated parameter (a_0) on the velocity profiles is presented in figure 14. It is revealed that the velocity enhances with increasing exponential accelerated parameter. The case $a_0 = 0$ corresponds to an impulsively started plate.

From figures 7-14 we observe that the velocity attains maximum values in the vicinity of the plate and then approach to zero far away from the plate which are identical with the imposed boundary conditions of velocity in equation (12). Hence both the graphical and mathematical results are found in excellent agreement.

Figure 15 displays dimensionless rate of heat transfer Nusselt number (Nu) against time t. This figure shows that increasing Prandtl number (Pr) and Newtonian heating parameter (γ) enhance the heat transfer coefficient. This may be explained by the fact that frictional forces become dominant with increasing values of Pr and yield greater heat transfer rate. Furthermore, as time advances, the value of Nu is decreasing and after some time it becomes constant. Nusselt number decreases on increasing radiation parameter (R) which implies that radiation tends to reduce rate of heat transfer at the plate. Wall temperature gradient is positive for all values of the Prandtl number. Physically it means that the heat is always transferred from the ambient fluid to the surface.

From figure 16, it is observed that the Sherwood number which determines the rate of mass transfer at the surface increases with increasing Schmidt number (Sc) and chemical reaction parameter (□), while reverse happens for increasing time values of t. Since increase in Sc means decrease in molecular diffusivity this in turn gives rise to increase in Sherwood number as Sherwood number is the ratio of convective and diffusive mass transfer coefficient. Chemical reaction parameter increases the interfacial mass transfer, so Sherwood number increases with an increase in □. It

is also noted that wall concentration gradient is positive for all values of the Schmidt number. Physically it means that the mass is always transferred from the ambient fluid to the surface.

Variations of skin friction (□) verses time are plotted in figures 17 - 19 for various parameters of interest. Figure 17 elucidates that with increasing Prandtl number (Pr) and modified Grashof number (Gm) frictional shear stress decreases while reverse happens for increasing Grashof number (Gr). The skin friction falls with an increase in Pr because an increase in the Prandtl number is due to increase in the viscosity of the fluid, which makes the fluid thick and hence a decrease in the velocity of the fluid therefore skin friction decreases with increasing Pr. Figure 18 illustrates the influence of radiation parameter (R), Schmidt number (Sc) and exponentially accelerated parameter (a_0) on skin friction profiles. It is noticed that skin friction increases with increasing values of Sc as it is higher for Sc = 0.66 in comparison to Sc = 0.22. Physically, it is correct since an increase in Sc serves to increase the momentum boundary layer thickness. Similar effects are shown by increasing radiation parameter and exponentially accelerated parameter. The effect of Casson parameter (□) and Newtonian heating parameter (□) on skin friction profiles (□) are presented in figure 19. By increasing the values of Casson parameter the values of the skin friction coefficient decreases but it increases upon increasing Newtonian heating parameter (□)

The present analytical (Laplace transform) solutions provide other researchers with solid benchmarks for numerical comparisons. The authors have used this method in other articles where they have bench marked approximate methods such as numerical, asymptotic or experimental methods against analytical (Laplace transform) solutions. The solution of the problem introduced new inverse Laplace transforms of exponential forms which are not available in the literature. These formulas are derived and are provided in the solution. Further, all these graphical results discussed above are in good agreement with the imposed boundary conditions given by (12). Hence, this ensures the accuracy of our results.

Nomenclature

C_p Specific heat at constant pressure, C^* Species concentration in the fluid, C_w^* Species concentration near the plate, C_∞^* Species concentration in the fluid far away from the plate, C(y,t) Dimensionless concentration, D Mass diffusivity, g Magnitude of the acceleration due to gravity, h Heat transfer coefficient, k Thermal conductivity of the fluid, k^* Mean absorption coefficient, r Thermal Grashof number, Gm Modified Grashof number, Pr Prandtl number, q_r Radiative heat flux in the y^* direction, R Radiation parameter, Sc Schmidt number, T^* Temperature of the fluid, T_∞^* Ambient temperature, t^* Time, t Non-dimensional time, u^* Dimensional velocity along x^*-direction, u(y,t) Dimensionless velocity, y^* Cartesian coordinate normal to the plate, y Dimensionless coordinate axis normal to the plate

GREEK SYMBOLS

α Chemical reaction parmeter , □ Casson parameter, β_t Volumetric Coefficient of thermal expansion, β_c Volumetric Coefficient of mass expansion, □ Newtonian heating parameter, ρ Density of the fluid, θ Dimensionless temperature, μ Coefficient of viscosity, ν Kinematic viscosity,

σ Stefan-Boltzmann constant, τ^* Skin-friction, τ Dimensionless skin-friction

REFERENCES:

[1] Mukhopadhyay S, Vajravelu K. "Effects of transpiration and internal heat generation/absorption on the unsteady flow of a Maxwell fluid at a stretching surface", ASME Journal of Applied Mechanics, 79, 044508, 2012, http://dx.doi.org/10.1115/1.4006260.

[2] Aksoy Y, Pakdemirli M, Khalique CM. " Boundary layer equations and stretching sheet solutions for the modified second grade fluid", International Journal of Engineering Sciences, 45, 829–41, 2007.

[3] Hayat T, Awais M, Sajid M. " Mass transfer effects on the unsteady flow of UCM fluid over a stretching sheet", Int J Mod Phys B, 25, 2863–78, 2011.

[4] Casson N. " A flow equation for the pigment oil suspensions of the printing ink type", Rheology of Disperse Systems, Pergamon, NewYork, USA, pp. 84–102, 1959.

[5] Fung YC. "Biodynamics circulation", Springer-Verlag, New York Inc., 1984.

[6] Dash RK, Mehta KN, Jayaraman G. "Casson fluid flow in a pipe filled with a homogeneous porous medium", International Journal of Engineering Sciences, 34(10), 1145–56, 1996.

[7] Mustafa M., Hayat t., Pop I., and Aziz A. "Unsteady boundary layer flow of a Casson fluid due to an impulsively started moving flat plate", Heat Transfer—Asian Research, 40(6), 563–576, 2011.

[8] Mukhopadhyay S. "Casson fluid flow and heat transfer over a nonlinearly stretching surface", Chinese Physics B, 22(7), Article ID 074701, 2013.

[9] Mukhopadhyay S. " Effects of thermal radiation on Casson fluid flow and heat transfer over an unsteady stretching surface subjected to suction/blowing", Chinese Physics. B, 22(11), Article ID 114702, 2013.

[10] Mukhopadhyay S., De P. R., Bhattacharyya K., Layek G.C. "Casson fluid flow over an unsteady stretching surface", Ain Shams Engineering Journal, 4, 933–938, 2013.

[11] Bhattacharya K., Hayat T., Alsaedi A. " Exact solution for boundary layer flow of casson fluid over a permeable stretching/Shrinking sheet", ZAMM-Journal of Applied Mathematics & Mechanics, 94(6), 522-528, 2014.

[12] Bhattacharya K "Boundary layer stagnation-point flow of casson fluid and heat transfer towards a shrinking/stretching sheet", Frontiers in Heat and Mass Transfer, 4(2), Article ID 023003, 2013

[13] Hossain, M.A., Alim, M.A. and Rees, D.A.S. "The effect of radiation on free convection from a porous vertical plate", International Journal of Heat and Mass Transfer, 42, 181-191, 1999.

[14] Raptis, A. and Perdikis, C., "Radiation and free convection flow past a moving plate", Applied Mechanics and Engineering, 4(4), 817-821, 1999.

[15] Soundalgekar, V.M., Das, U.N. and Deka, R.K. "Radiation effect on flow past an impulsively started vertical plate - An exact solution", Journal of Theoretical and Applied Fluid Mechanics, 1, 111-115, 1996.

[16] M. A. Hossain and H. S. Takhar , "Radiation Effects on mixed convection along a vertical plate with uniform surface temperature", Heat and Mass Transfer, 31(4), 243-24, 1996.

[17] Makinde, O.D. "Free convection flow with thermal radiation and mass transfer past a moving porous plate", International Communication in Heat and Mass Transfer, 32(10), 1411-1419, 2005.

[18] Muthucumaraswamy, R. and Chandrakala, P. "Effects of thermal radiation on moving vertical plate in the presence of an optically thin gray gas", Forschung im Ingenieurwese– Engineering Research, 69(4), 205-208, 2005.

[19] Muthucumaraswamy, R. "Exact solution of thermal radiation on vertical oscillating plate with variable temperature and mass flux", Theoreical and Appllied Mechanics, 37(1), 1-15, 2010.

[20] Deka, R. K. and Das, S. K. "Radiation effects on free convection flow near a vertical plate with ramped wall temperature" Engineering, 3, 1197-1206, 2011.

[21] Jana, R. N. and Ghosh, S.K. "Radiative heat transfer of an optically thick gay gas in the presence of indirect natural convection" World Journal of Mechanics, 1, 64-69, 2011.

[22] Pramanik S. "Casson fluid flow and heat transfer past an exponentially porous stretching surface in presence of thermal radiation", Ain Shams Engineering Journal, 5(1), 205–212, 2014.

[23] Shehzad S. A., Hayat T., Qasim M., Asghar S. "Effects of mass transfer on MHD flow of Casson fluid with chemical reaction and suction", Brazilian Journal of Chemical Engineering, 30(1), 187 – 195, 2013.

[24] Das U.N., Deka R., and Soundalgekar V.M. "Effect of Mass transfer on flow past an impulsively started infinite vertical plate with constant heat flux and chemical reaction", Forschung im ingenieurwesen/Engineering Research, 60(10), 284-287, 1994

[25] Jain Preeti "Combined influence of Hall current and Soret effect on chemically reacting magneto-micropolar fluid flow from radiate rotating vertical surface with variable suction in slip-flow regime", ISRN Mathematical Analysis, Article ID 102413, 23 pages, 2014 http://dx.doi.org/10.1155/2014/102413

[26] Makanda G., Shaw S., and Sibanda P. "Diffusion of Chemically Reactive Species in Casson Fluid Flow over an Unsteady Stretching Surface in Porous Medium in the Presence of a Magnetic Field", Mathematical Problems in Engineering, Hindawi publishing corporation, Article ID 724596.

[27] Merkin, J.H. "Natural convection boundary-layer flow on a vertical surface with Newtonian heating". Int. J. Heat Fluid Flow, 15, 392-398, 1994.

[28] Lesnic, D.,Ingham, D.B. and Pop, I. "Free convection boundary layer flow along a vertical surface in a porous medium with Newtonian heating" International Journal of Heat Mass Transfer,42, 2621-2627, 1999.

[29] Ibid "Free convection from a horizontal surface in porous medium with Newtonian heating" J. Porous Media, 3, 227-235, 2000.

[30] Lesnic, D., Ingham, D.B., Pop, I. and Storr, C. "Free convection boundary layer flow above a nearly horizontal surface in porous medium with Newtonian heating" Heat and Mass Transfer, 40 (4), 665-672, 2003.

[31] Chaudhary, R.C., Jain, Preeti "Unsteady free convection boundary-layer flow past an impulsively started vertical surface with Newtonian heating", Romanian Journal of Physics, 51, 911-925, 2006.

[32] Chaudhary, R.C., Jain, Preeti "An exact solution to the unsteady free convection boundary-layer flow past an impulsively started vertical surface with Newtonian Heating", Journal of Engineering Physics and Thermophysics, 80, 954-960, 2007.

[33] Jain Preeti and Chaudhary R. C. "Closed form solution of heat and mass transfer past an inclined oscillating surface with Newtonian heating under the effect of thermal radiation and mass diffusion", Advances in Applied Science Research, 4(6), 285-306, 2013.

[34] Narahari, M., Nayan, M.Y. "Free convection flow past an impulsively started infinite vertical plate with Newtonian Heating in the presence of thermal radiation and mass diffusion", Turkish Journal of Engineering and Environmental Sciences, 35,187-198, 2011.

[35] Raju, K.V.S., Reddy, T.S., Raju, M.C. and Venkataramana, "Free convective heat and mass transfer transient flow past an exponentially accelerated vertical plate with Newtonian heating in the presence of radiation", International Journal of Mathematics and Computer Application Research, 3(2), 215-226, 2013.

[36] Narahari, M. and Ishak, A. **"**Radiation effects on free convection flow near a moving vertical plate with Newtonian Heating", Journal of Applied Sciences, 11(7), 1096-1104, 2011.

[37] Hussanan A., Khan H., Sharidan S. "An exact analysis of heat and mass transfer past a vertical plate with Newtonian heating", Journal of Applied Mathematics, 2013, Article ID 434571,9 pages, 2013.

[38] Mebine, P., Adigio, E.M. "Unsteady free convection flow with thermal radiation past a vertical porous plate with Newtonian heating", Turkish Journal of Physics, 33, 109-119, 2009.

[39] R. Siegel and J. R. Howell "Thermal Radiation Heat Transfer", Taylor & Francis, New York, USA, 4th edition, 2002.

[40] Salleh, M. Z., Nazar, R. and I. Pop "Boundary layer flow and heat transfer over a stretching sheet with Newtonian heating", Journal of the Taiwan Institute of Chemical Engineers, 41(6), 651–655, 2010.

[41] Kasim, A. R. M., Mohammad, N. F., Aurangzaib, and Sharidan, S. "Natural convection boundary layer flow of a visco-elastic fluid on solid sphere with Newtonian heating", World Academy of Science, Engineering and Technology, 64, 628–633, 2012.

[42] R. Siegel and J. R. Howell "Thermal Radiation Heat Transfer", Taylor & Francis, New York, USA, 4th edition, 2002.

Figure 1:Temperature profiles for different values of Radiation parameter R when t = 0.2, Pr = 0.71 and $\gamma = 1$.

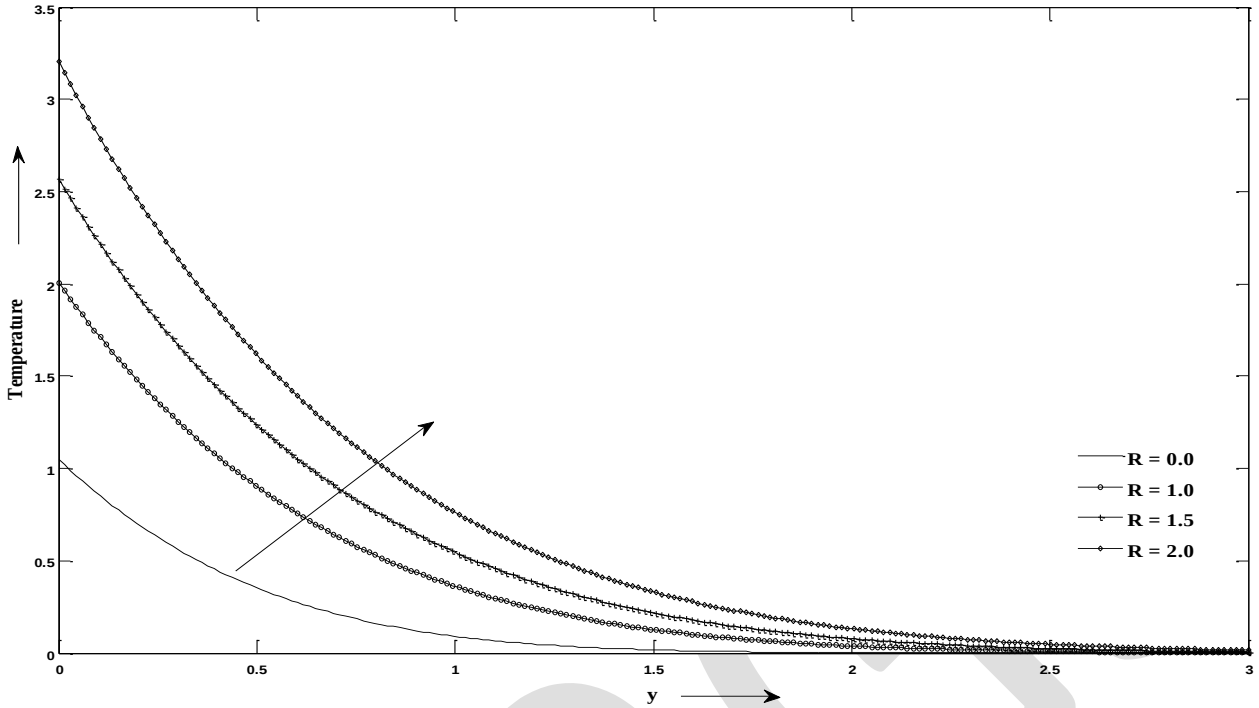

Figure 2: Temperature profiles for different values of time t when R = 1, Pr = 0.71 and $\gamma = 1.0$.

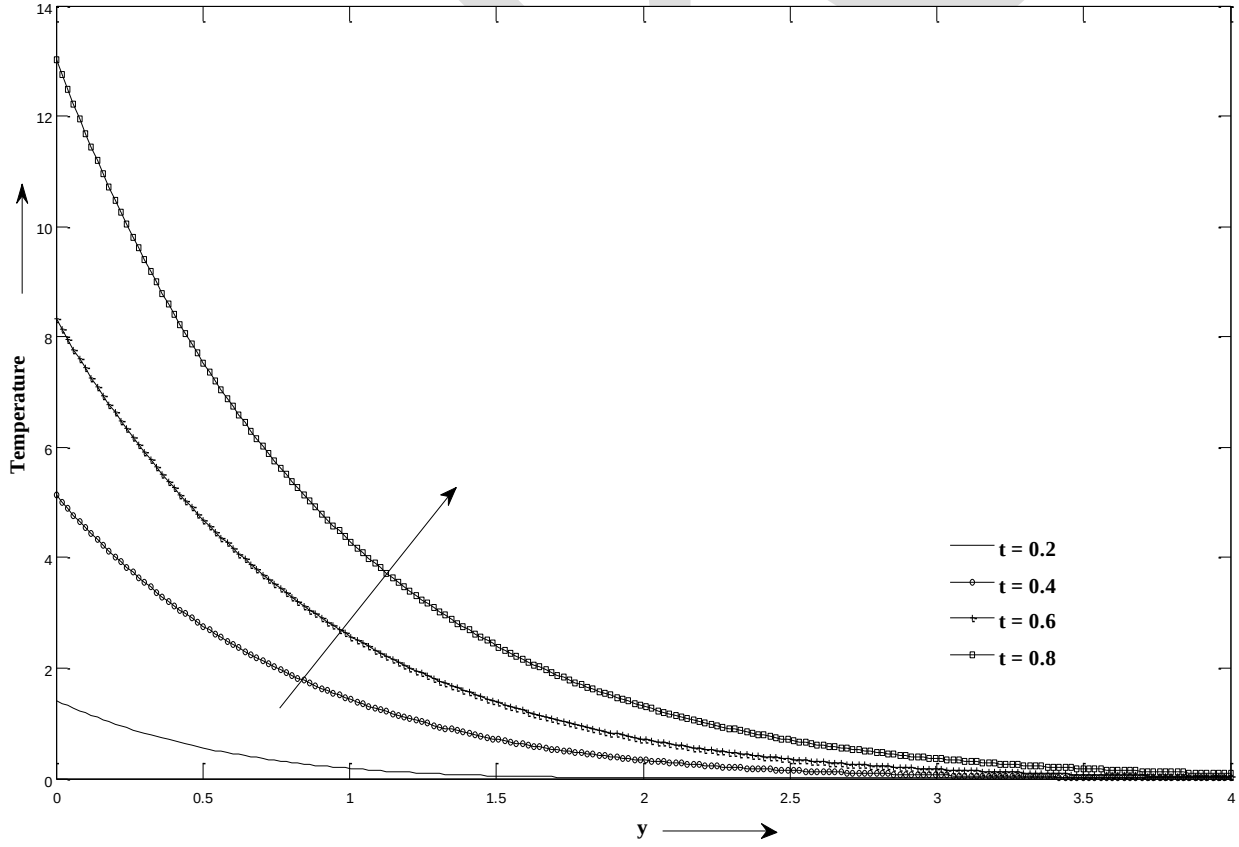

Figure 3 :Temperature profiles for different values of Prandtl number Pr when R = 2, t =0.4 and γ = 0.1

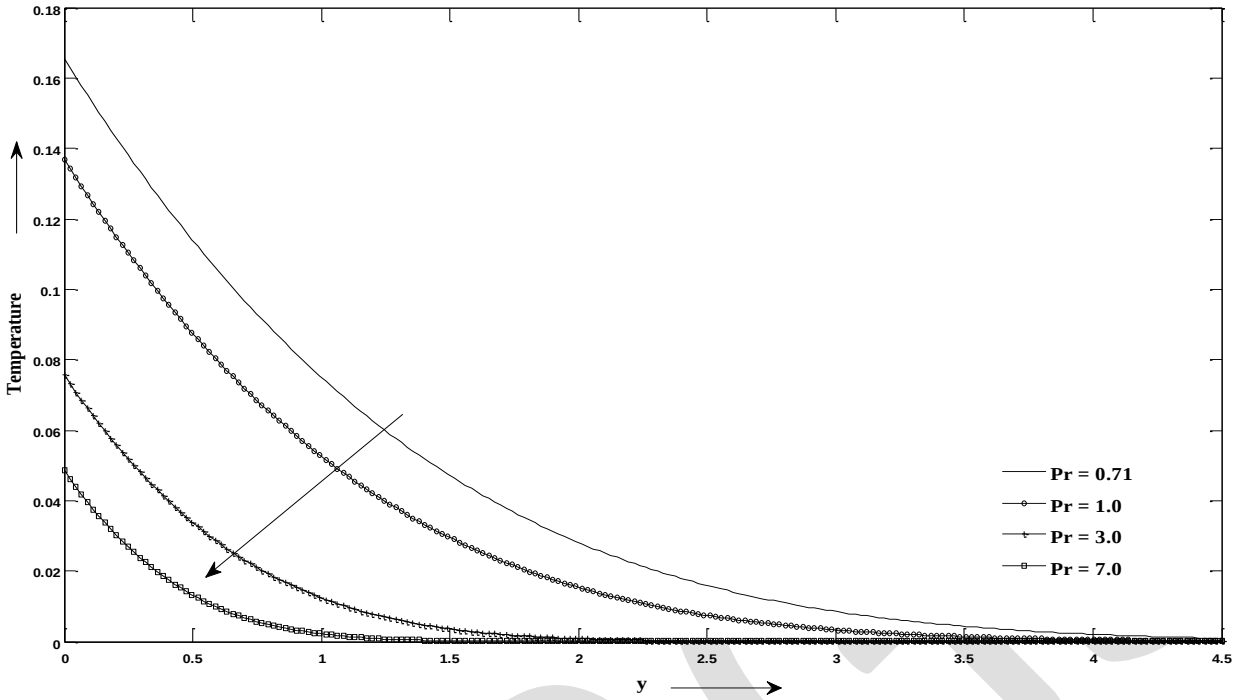

Figure 4 : Temperature profiles for different values of Newtonian Heating parameter when Pr = 0.71, R = 2 and t =0.2.

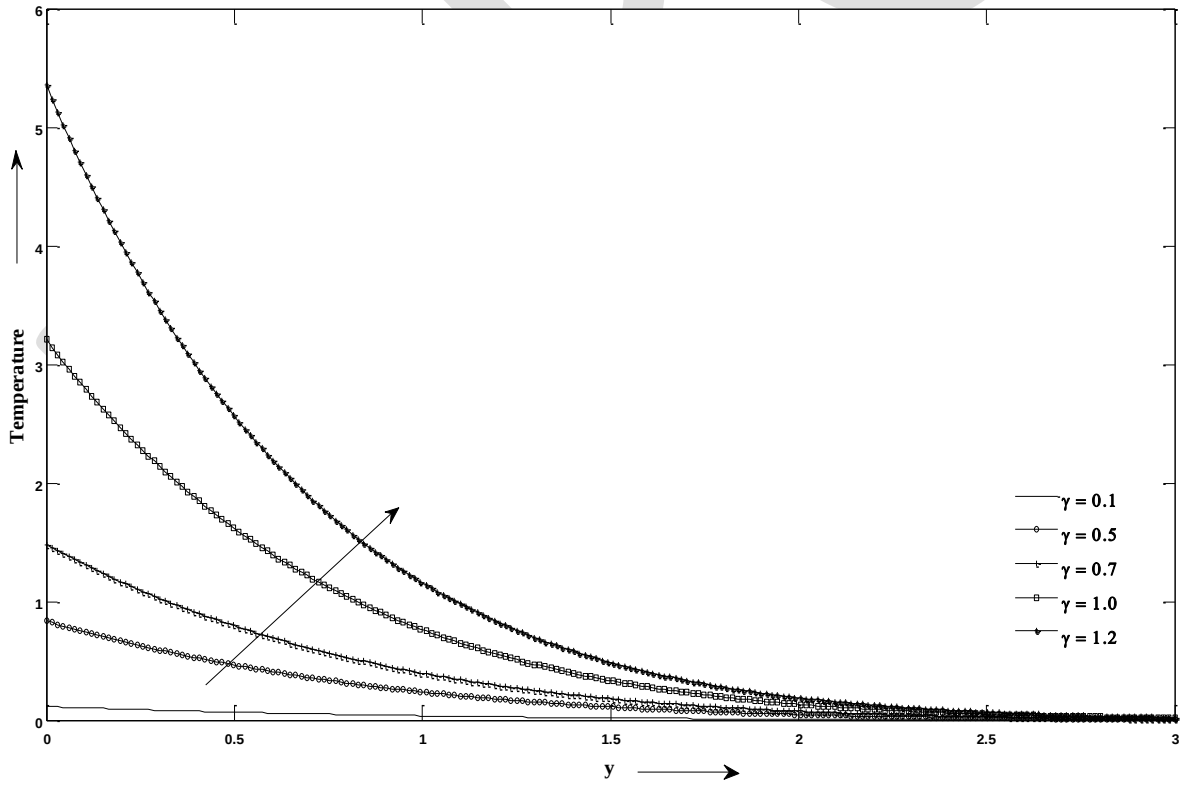

Figure 5: Concentration profiles for different values of Chemical reaction parameter when Sc = 0.66 and t = 0.4.

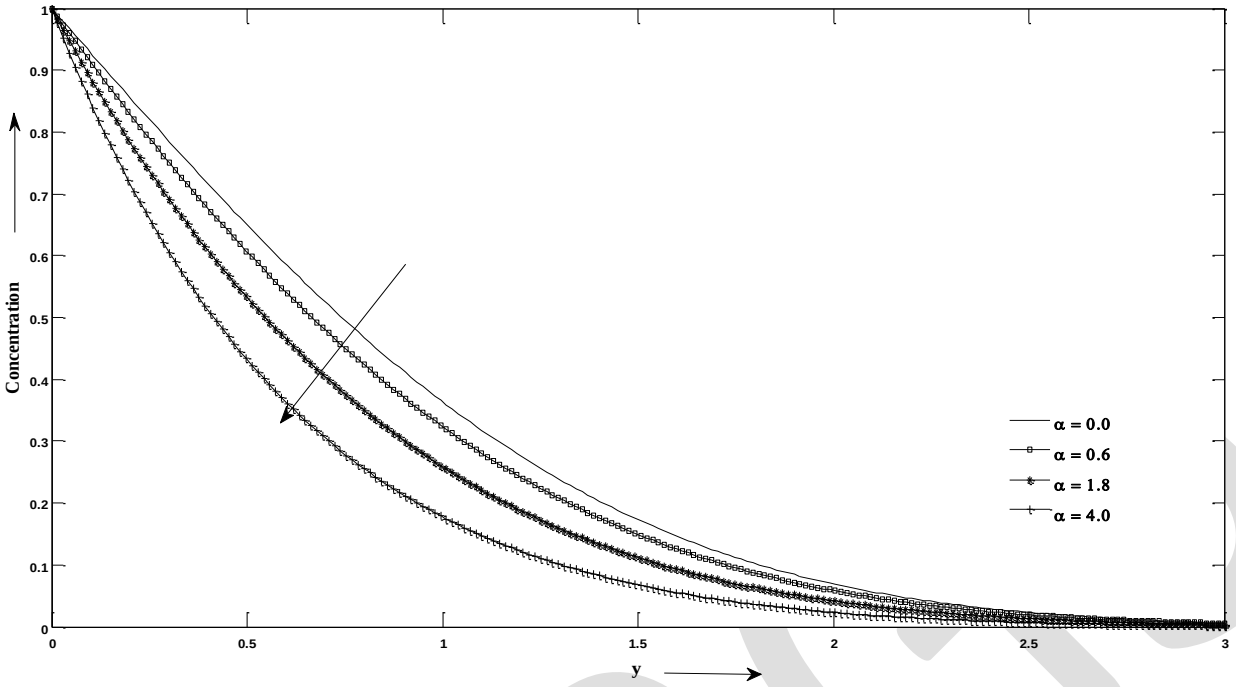

Figure 6 : Concentration profiles for different values of Schimdt number (Sc) and time (t) when $\alpha = 0.6$

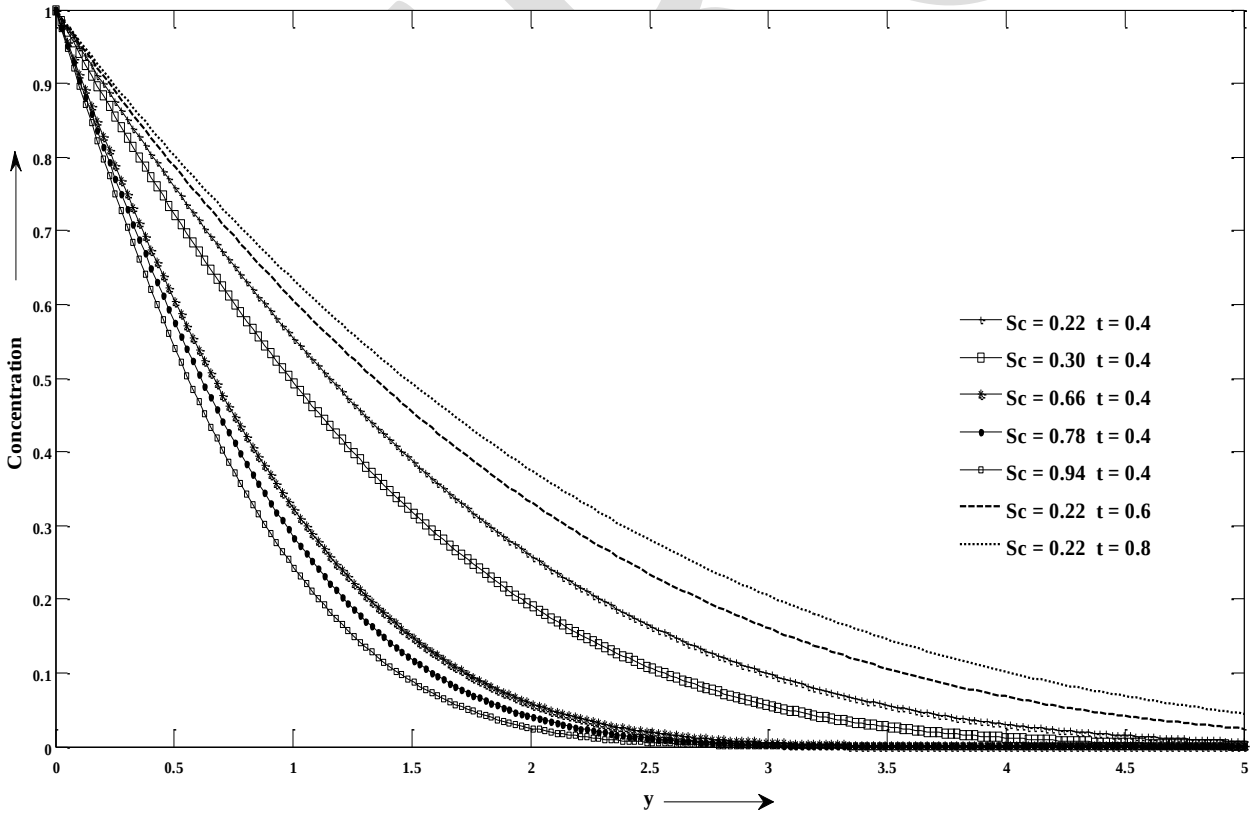

Figure 7 : Velocity profiles for different values of Grashoff number (Gr) and Modified Grashoff number (Gm) when t = 0.4, Pr = 0.71, Sc = 0.66, R = 2, ao = 1.5, α = 0.6, β = 2, γ = 1.

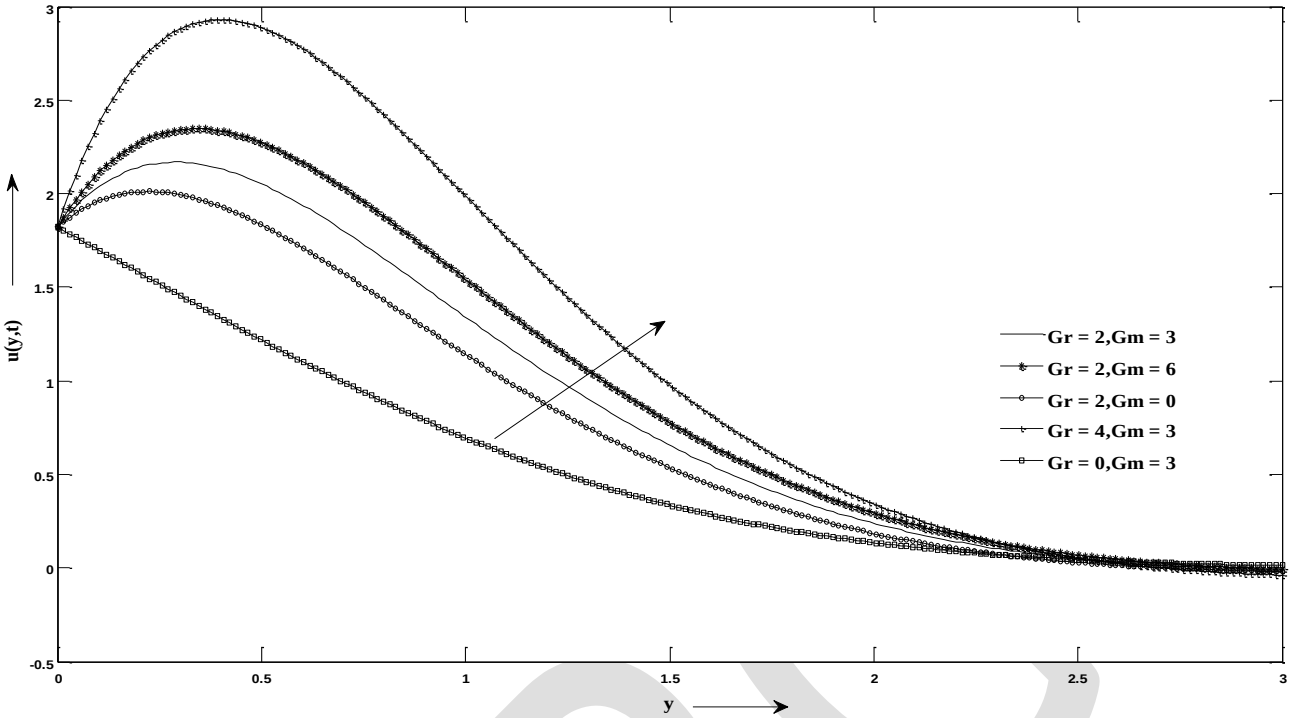

Figure 8: Velocity profiles for different values of Radiation parameter (R) when t = 0.4, Pr = 0.71, Sc = 0.66, Gr = 2, Gm = 3, ao = 1.5, α = 0.6, β = 2, γ = 1.

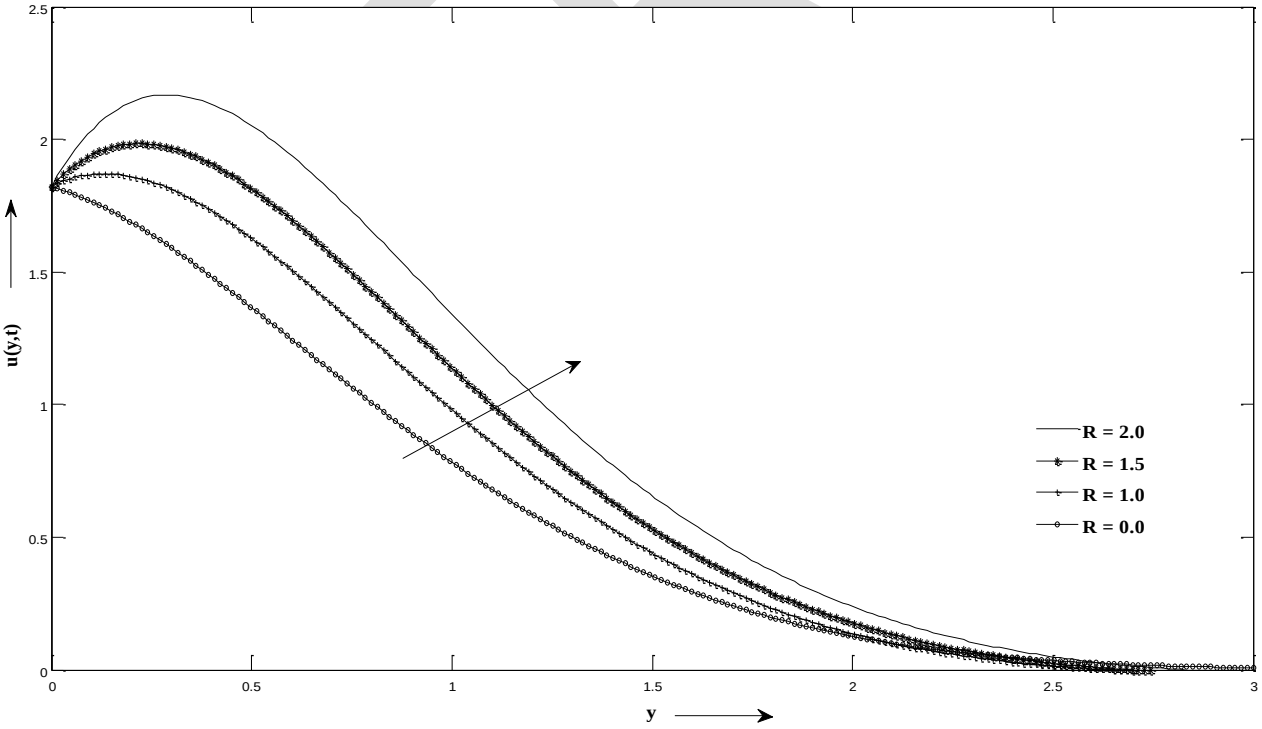

Figure 9: Velocity profiles for different values of Casson parameter when t = 0.1, Pr = 0.71, Sc = 0.66, Gr = 2, Gm = 3, ao = 1.5, R = 2, $\alpha = 0.6, \gamma = 1$.

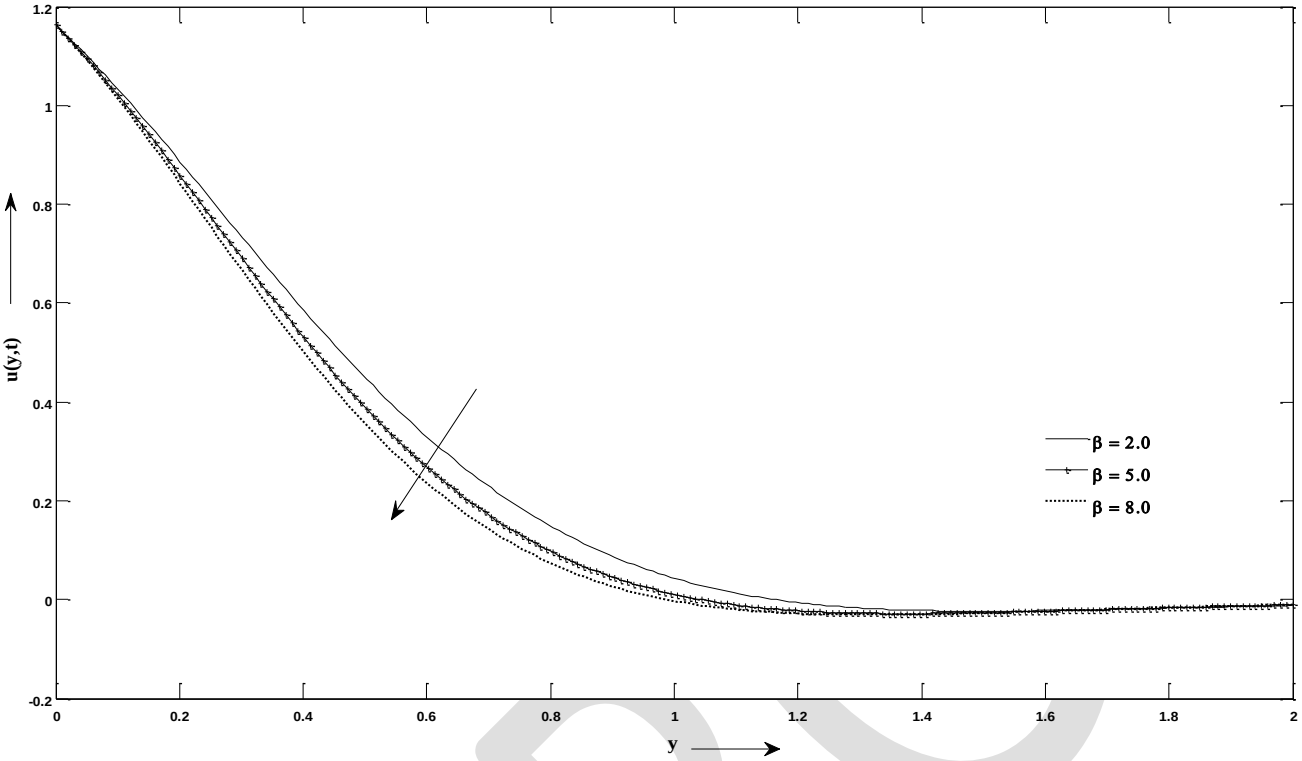

Figure 10: Velocity profiles for different values of Schimdt number (Sc) when t = 0.4, Pr = 0.71, Gr = 2, Gm = 3, Sc = 0.66, R = 2, ao = 0.5, $\alpha = 1.6, \beta = 2, \gamma = 1$.

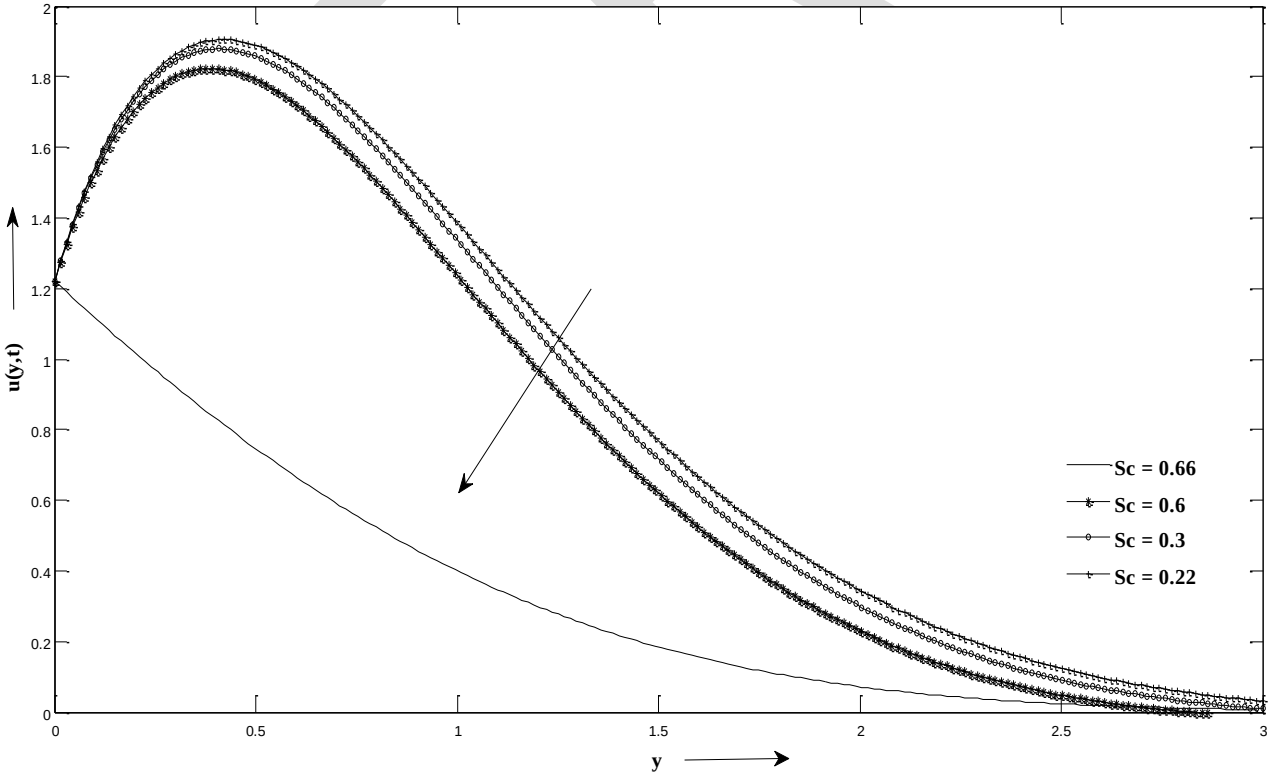

Figure 11 : Velocity profiles for different values of Prandtl number (Pr) and time (t) when Gr = 2, Gm = 5, Sc = 0.66, R = 2, ao = 0.5, α = 0.6, β = 2, γ = 1.

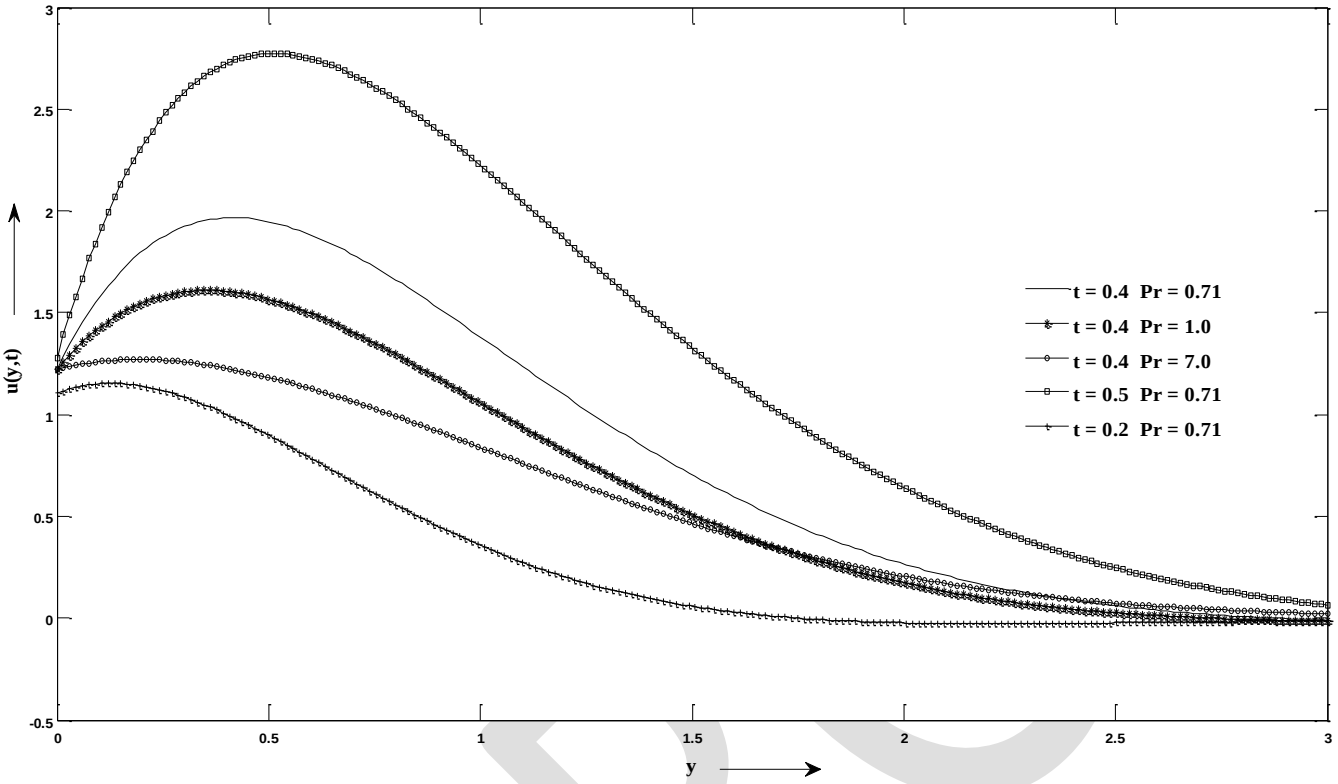

Figure 12: Velocity profiles for different values of Newtonian Heating parameter when t = 0.4, Pr = 0.71, Gr = 2,Gm = 3, Sc = 0.66, ao = 1.5, R = 2, α = 0.6, β = 2.

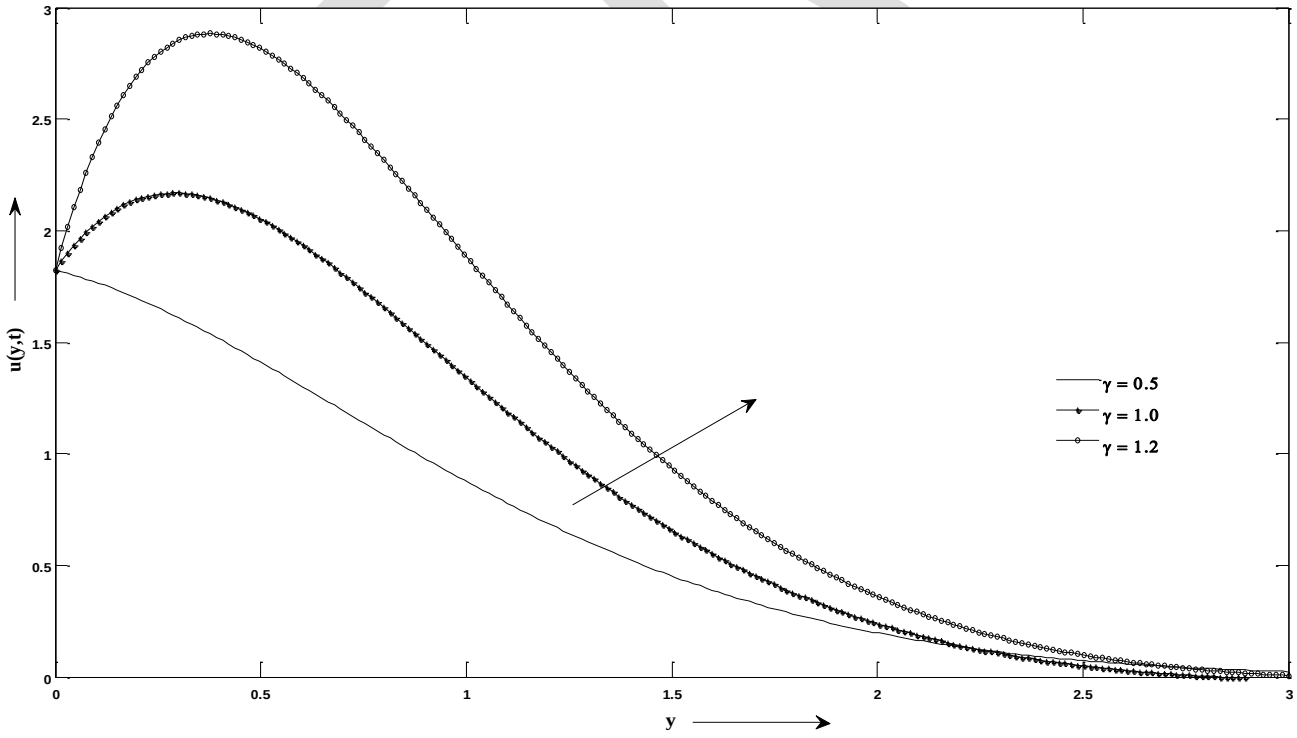

Figure 13: Velocity profiles for different values of chemical reaction parameter when t = 0.4, Pr = 0.71, R = 2, ao = 1.5, Gr = 5, Gm = 5, Sc = 0.66, β = 4, γ = 1.

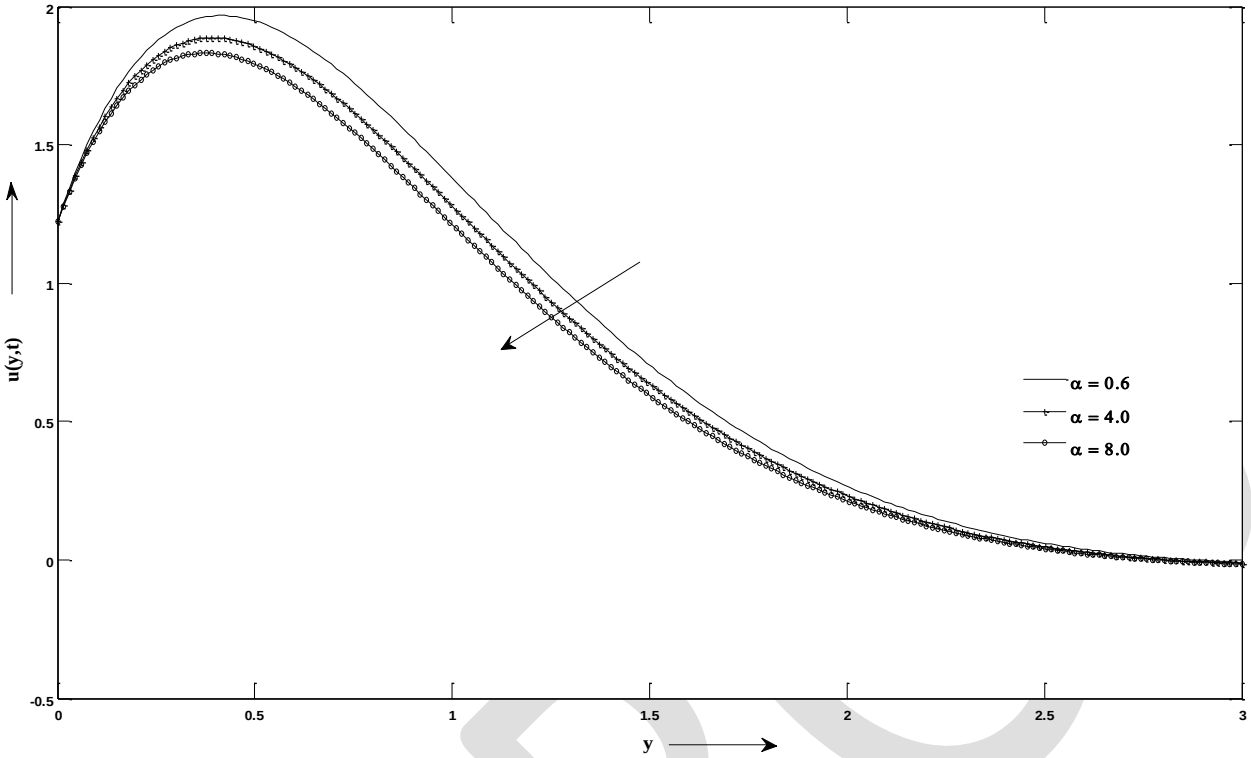

Figure 14: Velocity profiles for different values of exponential accelerated parameter (ao) when t = 0.4, Pr = 0.71, Sc = 0.66, Gr = 2, Gm = 3, R = 2, α = 0.6, β = 2, γ = 1.

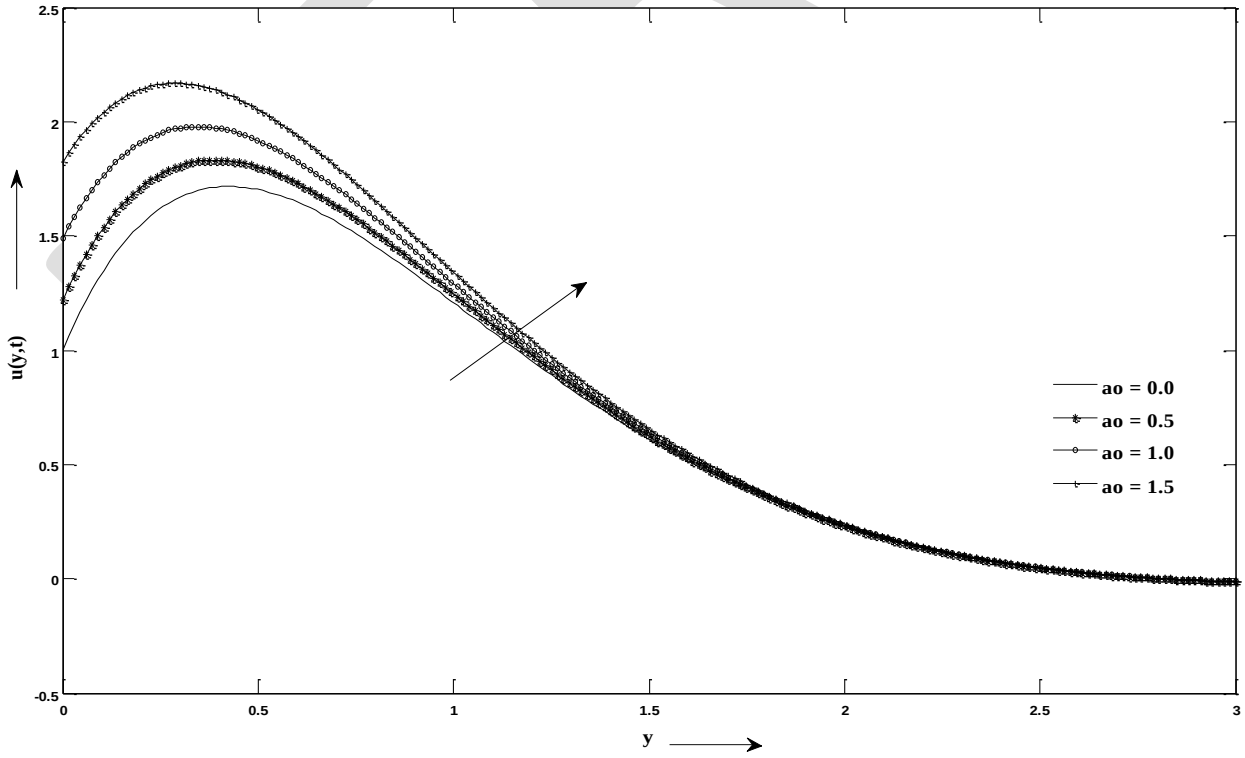

Figure 15: Variation of Nusselt number for different values of Prandtl number (Pr), radiation parameter (R), Newtonian heating Parameter (γ).

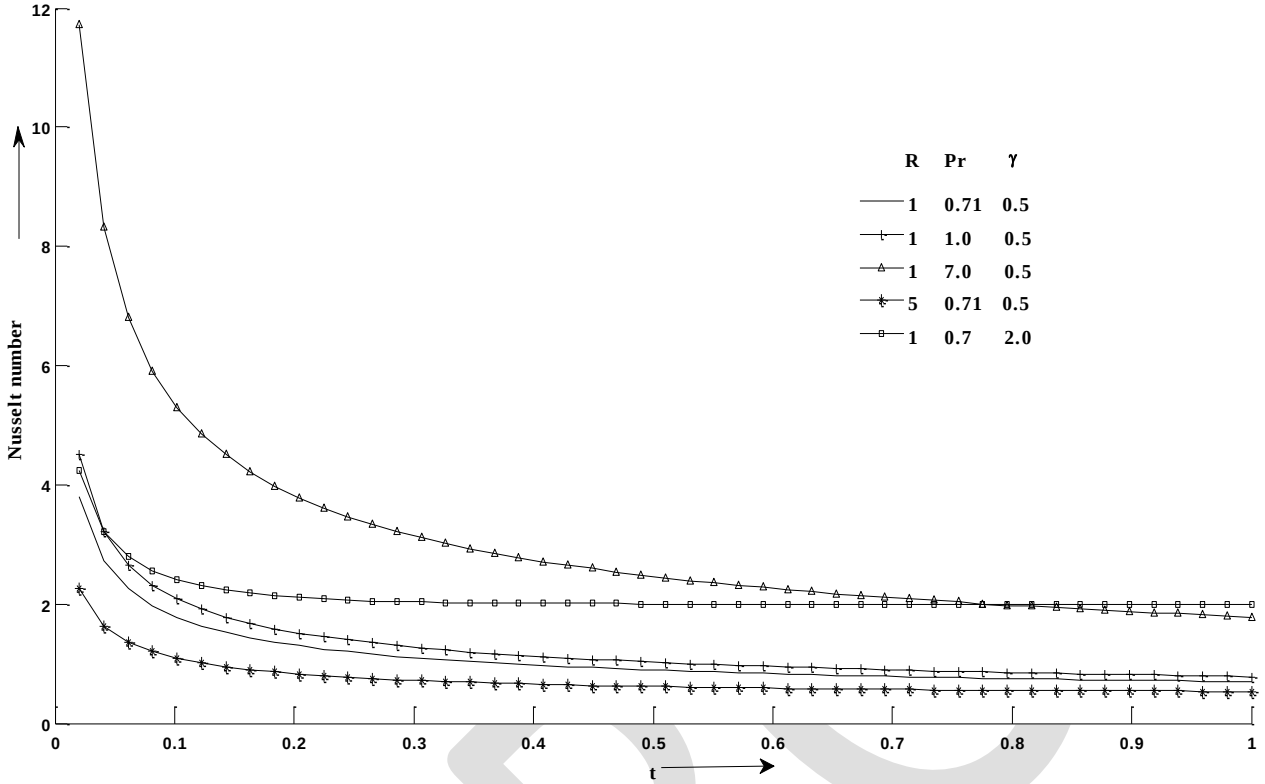

Figure 16: Sherwood number for different values of Schmidt number and Chemical Reaction parameter.

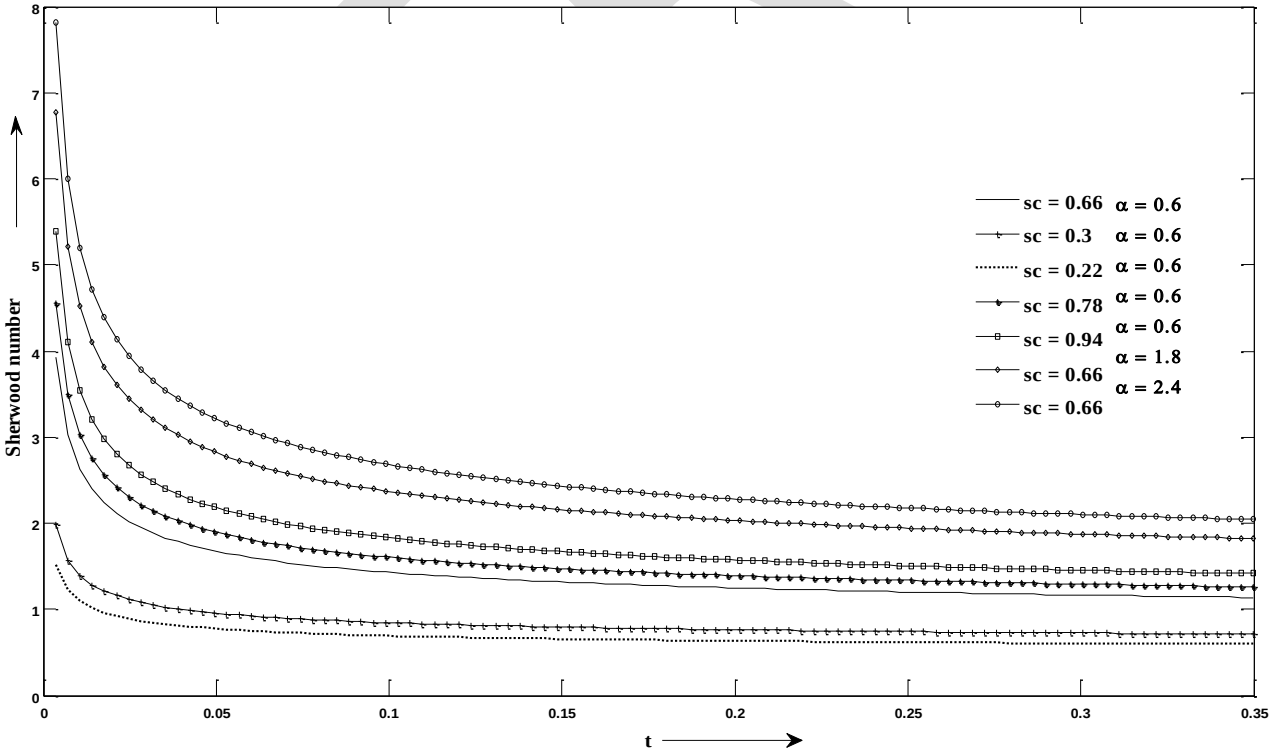

Figure 17 : Skin friction profiles when Sc = 0.66, R = 2, ao = 0.5, α = 0.6, β = 2, γ = 1.

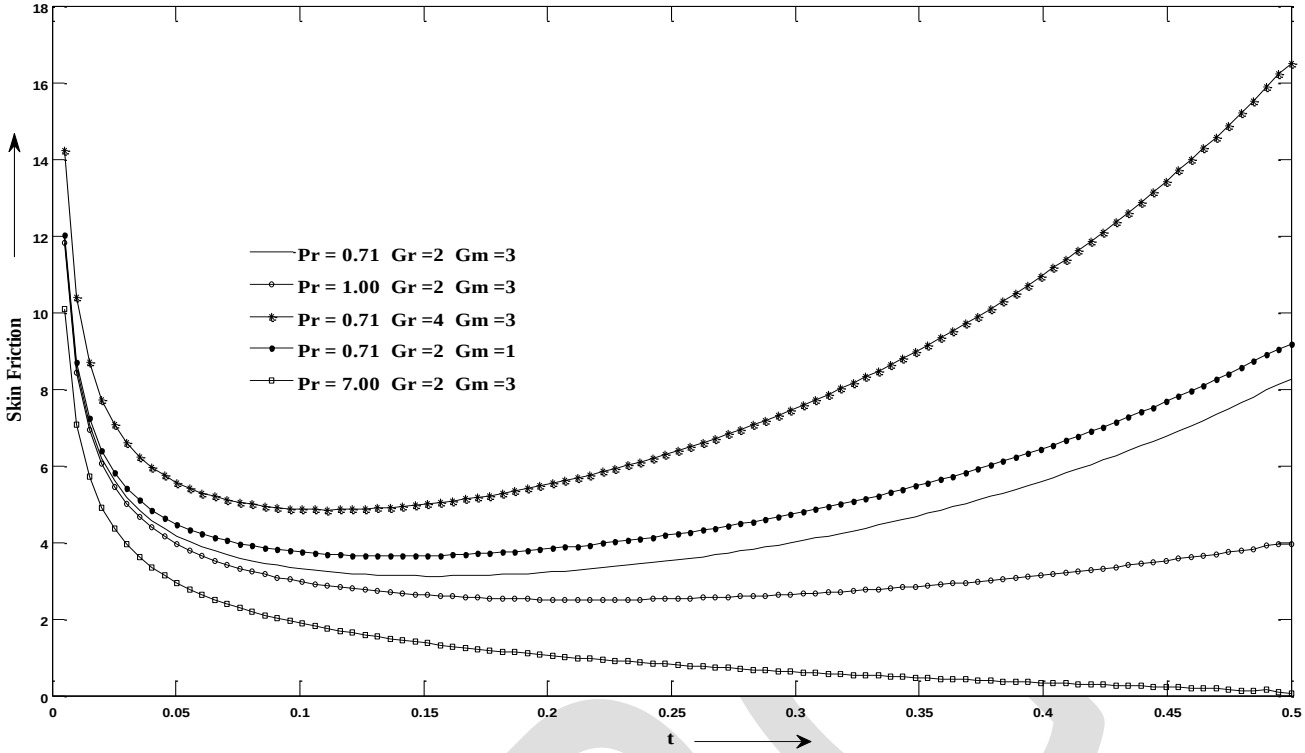

Figure 18 : Skin friction profiles when Pr = 0.71, Gr = 2, Gm = 3, α = 0.6, β = 2, γ = 1.

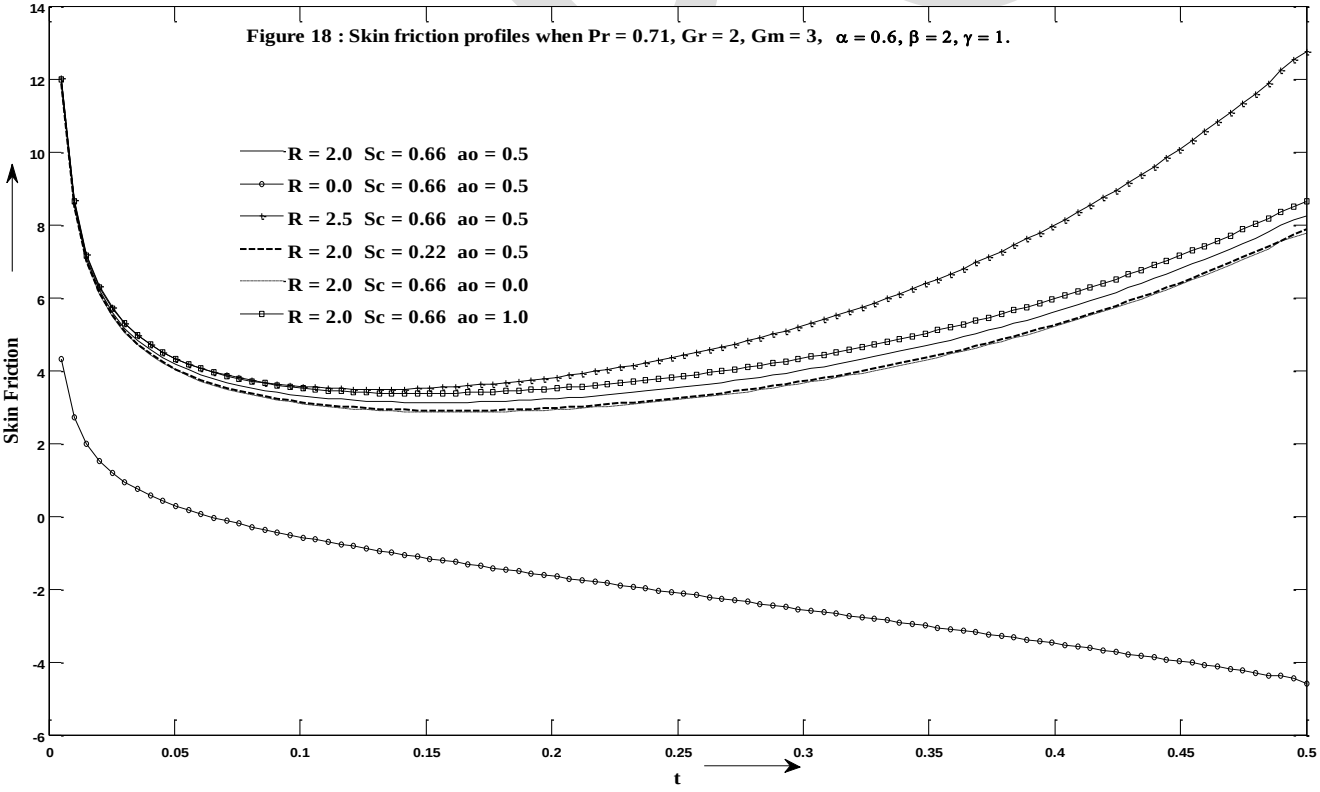

Figure 19 : Skin friction profiles when Pr = 0.71, Gr = 2, Gm = 3, Sc = 0.66, R = 2, ao = 0.5, α = 0.6.